DEVELOPMENT OF A SIMPLIFIED THERMAL ANALYSIS PROCEDURE FOR INSULATING GLASS UNITS

A Thesis

by

JEREMY WAYNE KLAM

Submitted to the Office of Graduate Studies of
Texas A&M University
in partial fulfillment of the requirements for the degree of

MASTER OF SCIENCE

August 2007

Major Subject: Civil Engineering

DEVELOPMENT OF A SIMPLIFIED THERMAL ANALYSIS PROCEDURE FOR INSULATING GLASS UNITS

A Thesis

by

JEREMY WAYNE KLAM

Submitted to the Office of Graduate Studies of
Texas A&M University
in partial fulfillment of the requirements for the degree of

MASTER OF SCIENCE

Approved by:

Chair of Committee, W. Lynn Beason
Committee Members, Terry Kohutek
Bryan Maggard
Head of Department, David Rosowsky

August 2007

Major Subject: Civil Engineering

ABSTRACT

Development of a Simplified Thermal Analysis Procedure
for Insulating Glass Units. (August 2007)
Jeremy Wayne Klam, B.S., Texas A&M University
Chair of Advisory Committee: Dr. W. Lynn Beason

A percentage of insulating glass (IG) units break each year due to thermally induced perimeter stresses. The glass industry has known about this problem for many years and an ASTM standard has recently been developed for the design of monolithic glass plates for thermal stresses induced by solar irradiance. It is believed that a similar standard can be developed for IG units if a proper understanding of IG thermal stresses can be developed. The objective of this research is to improve understandings of IG thermal stresses and compare the IG thermal stresses with those that develop in monolithic glass plates given similar environmental conditions.

The major difference between the analysis of a monolithic glass plate and an IG unit is energy exchange due to conduction, natural convection, and long wave radiation through the gas space cavity. In IG units, conduction, natural convection, and long wave radiation combine in a nonlinear fashion that frequently requires iterative numerical analyses for determining thermal stresses in certain situations. To simplify the gas space energy exchange, a numerical propagation procedure was developed. The numerical propagation procedure combines the nonlinear effects of conduction, natural convection, and long wave radiation into a single value. Use of this single value closely approximates the nonlinear nature of the gas space energy exchange and simplifies the numerical analysis.

The numerical propagation procedure was then coupled with finite element analysis to estimate thermal stresses for both monolithic glass plates and IG units. It is shown that

the maximum thermal stresses that develop in IG units increase linearly with input solar irradiance during the transient phase. It is shown that an initial preload stress develops under equilibrium conditions due to the thermal bridge effects of the spacer. It is shown that IG units develop larger thermal stresses than monolithic glass plates under similar environmental conditions. Finally, it is shown that the use of low-e coatings increase IG thermal stresses and that the location of low-e coating as well as environmental conditions affect which glass plate develops larger thermal stresses.

ACKNOWLEDGEMENTS

The author wishes to thank Drs. W. L. Beason, T. L. Kohutek, and B. Maggard for the guidance and counsel given in the preparation of this thesis. The author also wishes to thank Mr. A. W. Lingnell, who provided technical input for the research presented herein.

NOMENCLATURE

α = Solar absorptance

α_D = Thermal diffusivity

α_T = Thermal coefficient of expansion

β = 1/Film_Temperature

ε_2 = Emissivity of surface number 2

ε_3 = Emissivity of surface number 3

ε = Emissivity

$\varepsilon_{EFFECTIVE}$ = Effective emissivity

λ = Wave length

μ = Viscosity

ρ = Solar reflectance

ρ_m = Mass density

σ = Stress

σ_{SB} = Steffan-Boltzmann constant

τ = Solar transmittance

υ = Kinematic viscosity

A = Area

Absorbtance_Outer = Absorbed solar irradiance of outer plate

Absorbtance_Inner = Absorbed solar irradiance of inner plate

CEEC = Cavity energy exchange coefficient

C_p = Specific heat

E = Young's modulus

Film_Temperature = Film temperature

g = Acceleration due to gravity

Gr = Grashof number

$h_{CONVECTION}$ = Convection coefficient

$h_{RADIATION}$ = Effective long wave radiation convection coefficient

h_{TOTAL} = Total convection coefficient

h_{TOTAL_CAVITY} = Total cavity energy exchange coefficient

h_{TOTAL_INDOOR} = Total indoor energy exchange coefficient

$h_{TOTAL\_OUTDOOR}$ = Total outdoor energy exchange coefficient

k = Thermal conductivity

k_{FLUID} = Thermal conductivity of fluid

L = Length

Nu = Nusselt number

q_{NET} = Net energy of outer/inner plate control volume

q_{NET_INNER} = Net energy of inner plate control volume

q_{NET_OUTER} = Net energy of outer plate control volume

P = Total error sum of squares

Pr = Prandtl number

q = Energy flow

Ra = Rayleigh number

Re = Reynolds number

T_1 = Temperature of surface number 1

T_2 = Temperature of surface number 2

T_3 = Temperature of surface number 3

T_4 = Temperature of surface number 4

ΔT = Change in temperature

T_{CGA} = Temperature of center of glass area

T_{ENV} = Temperature of environment

T_{GL} = Temperature of glass surface

$T_{HAT\_OUTER\_i}$ = Outer plate temperature at time i from CEEC method

$T_{HAT\_INNER\_i}$ = Inner plate temperature at time i from CEEC method

T_i = Temperature at time step i

T_{i+1} = Temperature at time step i+1

T_j = Temperature of surface j

T_k = Temperature of surface k

T_{INDOOR} = Temperature of the indoor environment

T_{INNER_i} = Inner plate temperature at time i from nonlinear method

$T_{OUTDOOR}$ = Temperature of the outdoor environment

T_{OUTER_i} = Outer plate temperature at time i from nonlinear method

T_{PG} = Perimeter of glass temperature

Δt = Time step size

t_{GL} = Thickness of glass

u = Free stream velocity

x = Distance from leading edge of plate

TABLE OF CONTENTS

LIST OF FIGURES

Page

Page

LIST OF TABLES

Page

CHAPTER I

INTRODUCTION

Windows serve many purposes and are an essential component in the commercial and residential built environment. Windows serve aesthetic purposes on the facade of buildings and allow a means for natural light and solar irradiance to enter the interior of a building. Windows improve the quality of the indoor environment by providing humans with a connection to the outdoors (Han and Muneer 1996). As the amount of time spent indoors has increased over the past century, windows have proven to increase the psychological health of humans, and improve the quality of the home and work environment, (Muneer et al. 2000).

Although windows are an essential component in the commercial and residential built environment, windows exchange more thermal energy with the environment than any other part of the building envelope (Muneer et al. 1996; Ismail and Hendriquez 2005). Originally, windows consisted of a single clear glass plate, referred to herein as a monolithic glass plate, that separated the indoor environment from the outdoor environment. In the early 1970's the use of insulating glass that incorporated two or three glass plates, separated by one or more gas spaces became more popular as the cost of heating and cooling increased. As the concern for energy conservation continues to grow, more stringent energy standards are being enforced to limit the amount of energy that can be exchanged between a building and the surrounding environment (ASHRAE 2005).

In an effort to meet new energy standards, high performance insulating glass (IG) units

---

This thesis follows the style of *Journal of Structural Engineering*.

have become essential in the residential and commercial built environment. The glass plates that make up a high performance IG unit can include various types and thicknesses of glass that incorporate different coatings and tints for both aesthetic and energy performance reasons. In addition, the high performance IG unit can incorporate different fill gases and spacers to improve energy performance. Windows that incorporate high performance IG units, have proven to be more energy efficient than monolithic windows in almost all applications.

As the use of IG units of all types have increased, empirical data suggest that the breakage of the IG glass plates due to thermal stresses has increased significantly when compared to windows that incorporate monolithic glass. Thermal stresses can be caused by any mechanism that inputs heat into the center area of the glass; however, it is widely believed that solar irradiance provides the most common heat mechanism that causes thermal breakage (Beason and Lingnell 2002). Therefore, this thesis is focused only on solar irradiance as a heat input mechanism for the development of thermal stress.

Thermal breakage of a glass plate occurs when a critical temperature difference develops between the center of glass area and the perimeter of the glass. This temperature difference leads to the development of thermal stresses along the perimeter of the glass (Turner 1977; Wright and Barry 1999; Zhong-wei et al. 1999; Pilkington 2005). If the perimeter stresses exceed the strength of the glass, breakage will result.

Significant efforts have been devoted to understanding thermal breakage in monolithic glass plates (Beason and Lingnell 2002). A simplified procedure that allows the user to estimate the design thermal stress as a function of applied solar irradiance and window frame type is presented in ASTM standard E 2431-06 (ASTM 2006). While, this procedure allows the variation of thermal stress with exposure to solar irradiance to be calculated for monolithic glass, the procedure is not applicable to IG units in its current form.

Even though IG units have become an integral component in the building environment, much less effort has been put forth to understand the development of thermal stresses in IG units than is the case with monolithic glass. The research presented in this thesis is intended to improve understandings of the development of thermal stresses in IG units and how these IG thermal stresses compare to those that develop in monolithic glass plates.

In the research reported herein, it is assumed that the energy exchange coefficients for the indoor and outdoor surfaces of an IG unit and a monolithic glass plate are the same when the windows are placed in the same environment. For a monolithic glass plate, energy is exchanged from the outdoor environment to the indoor environment through absorbed solar irradiance, conduction in the body of the glass, and convection and long wave radiation from the glass surfaces. This energy exchange also takes place in IG units; however, IG units incorporate an intermediate energy exchange through the gas space cavity that is not present with monolithic glass (ASHRAE 2005). This energy exchange through the IG gas space is controlled by conduction, natural convection, and long wave radiation. These three factors combine in a nonlinear fashion which greatly complicates heat exchange calculations (Wright 1996; Muneer et al. 1997).

The major objective of this thesis is to develop a method to determine a total energy exchange coefficient that can be used to closely model the energy transfer between the inner and outer glass plates of an IG unit. To accomplish this, a numerical propagation procedure has been developed that linearizes the total energy exchange across the gas space cavity of IG units with respect to outdoor and indoor glass plate temperatures. Application of the procedure results in the development of a single value, referred to herein as the cavity energy exchange coefficient (CEEC) that can be used to approximate the energy exchange through the gas space cavity. Use of this CEEC value greatly simplifies the thermal analysis of IG units (Rubin 1982; Han and Muneer 1996; Muneer et al. 2000; Gordon 2001).

The CEEC value is then coupled with finite element analysis to predict the variation of temperature difference between the center of glass area and the perimeter of glass for a set of cases involving both monolithic glass plates and IG units. These temperature differences are used to estimate the thermal stresses that develop along the glass perimeter. The thermal stresses that develop in the IG units are then compared to the thermal stresses that develop in monolithic glass plates and conclusions are drawn.

Chapter II presents a detailed problem statement. Chapter III presents a review of the pertinent literature which discusses energy exchange between windows and the surrounding environment. Chapter IV presents the numerical propagation procedure used to determine the CEEC. Chapter V couples the numerical propagation procedure with finite element analysis to examine the thermal performance of a selected set of monolithic glass plates and IG units. Chapter VI presents the conclusion of the research.

CHAPTER II

RESEARCH PROBLEM

It has long been understood that a significant amount of window glass breakage in both monolithic glass plates and insulating glass (IG) units is caused by thermally induced stresses. Thermal stresses occur when a temperature difference develops between the center of glass area and the perimeter of glass (Turner 1977; Wright and Barry 1999; Zhong-wei et al. 1999; Pilkington 2005). Significant efforts have been devoted to understanding thermal breakage in monolithic glass plates (Beason and Lingnell 2002; ASTM 2006). However, as new energy standards increase energy efficiency requirements, fewer windows incorporate monolithic glass plates. To satisfy the new energy efficiency requirements, IG units have become essential in most residential and commercial applications.

To develop an understanding of how thermal stresses develop in IG units, it is first necessary to understand the methodologies currently in place for the design of monolithic glass plates and how these methodologies relate to the design of IG units. If a monolithic glass plate is in equilibrium with the surrounding environment, the amount of energy input into the glass via solar irradiance is equal to the amount of energy lost to the surrounding environment via the heat transfer properties of conduction, convection, and long wave radiation from the interior and exterior surfaces of the monolithic glass plate.

Total energy exchange coefficients have been used in the design of monolithic glass plates to linearize the energy exchange between a monolithic glass plate and the surrounding environment (Beason and Lingnell 2002; ASHRAE 2005). These coefficients combine the effects of conduction, convection, and long wave radiation into a single value that can be used to model the energy exchange between a monolithic glass plate

and the indoor/outdoor environment. Standardized total energy exchange coefficients have recently been developed and incorporated into ASTM, E 2431-06 (Beason and Lingnell 2002; ASTM 2006). Implementation of the total energy exchange coefficients are illustrated in Fig. 1. The total energy exchange coefficients incorporated in ASTM, E2431-06 (ASTM 2006) are believed to represent a sheltered outdoor condition and a typical indoor energy exchange condition.

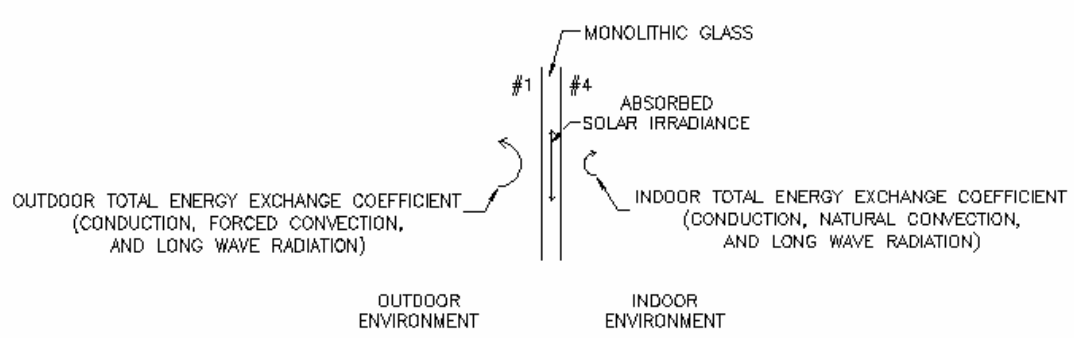

Fig. 1. Total energy exchange coefficients used in the design of monolithic glass plates

Use of the total energy exchange coefficients make it possible to estimate the variation of temperature between the center of glass area and the perimeter of glass for monolithic glass plates that are subjected to a given solar irradiance. It is generally accepted that the edge stresses that develop in the glass are proportional to the temperature difference between the center of glass area and the perimeter of glass (Wright and Barry 1999; Zhong-wei et al. 1999; Pilkington 2005).

A simplified procedure that allows the user to estimate the design thermal stress as a function of the applied solar irradiance and window frame type is presented in ASTM standard E 2431-06 (ASTM 2006). While this procedure allows the variation of thermal stress with exposure to solar irradiance to be calculated for monolithic glass, the procedure is not applicable to IG units in its current form. This is the case because IG units

incorporate energy exchange through gas space cavities (Raithby et al. 1982; Wright 1996; Muneer et al. 1997).

IG units consist of two or three glass plates that are separated by one or more gas spaces. By far the most common IG units consist of two rectangular glass plates separated by a single gas space (Muneer et al. 2000). Therefore, this research is focused on two plate IG units. Fig. 2, presents a sketch of a corner cut away of a two plate IG unit.

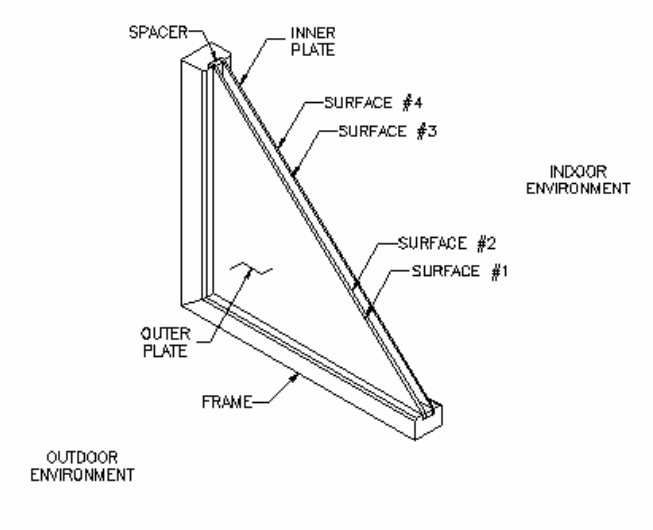

Fig. 2. Corner cut away of an IG unit

An IG unit, referred to in this research, is composed of two rectangular glass plates, the outer and inner plate, separated by one gas space. Surfaces number 1 (#1) and number 2 (#2) are associated with the outer plate, as shown in Fig. 2. The #1 surface is exposed to the outdoor environment and the #2 surface is exposed to the gas space cavity. Surfaces number 3 (#3) and number 4 (#4) are associated with the inner plate, as shown in Fig. 2. The #4 surface is exposed to the indoor environment and the #3 surface is exposed to the gas space cavity. Because of durability issues, low emissivity (low-e) coatings are typically applied to the #2 or #3 surface of IG units (ASHRAE 2005).

The primary components of an IG unit are the inner and outer glass plates, the spacer, the primary sealant, the secondary sealant, and the gas space desiccant as illustrated in Fig. 3. The spacer is the structural component placed between the outer and inner glass plates of the IG unit. The spacer keeps the gas space at a constant thickness and provides an adhesion surface for the primary and secondary sealants. The primary sealant is placed between the plates of an IG unit and the spacer to provide a seal between the gas space cavity and the surrounding environment. The secondary sealant is placed on the backside of the spacer joining the outer and inner glass plates of the IG unit. The secondary sealant is used to ensure protection from water and oils by providing a second seal and is the structural material that bonds the glass plates to the spacer. The gas space desiccant is used to absorb any moisture that has remained inside the gas space of the IG unit after construction (ASHRAE 2005).

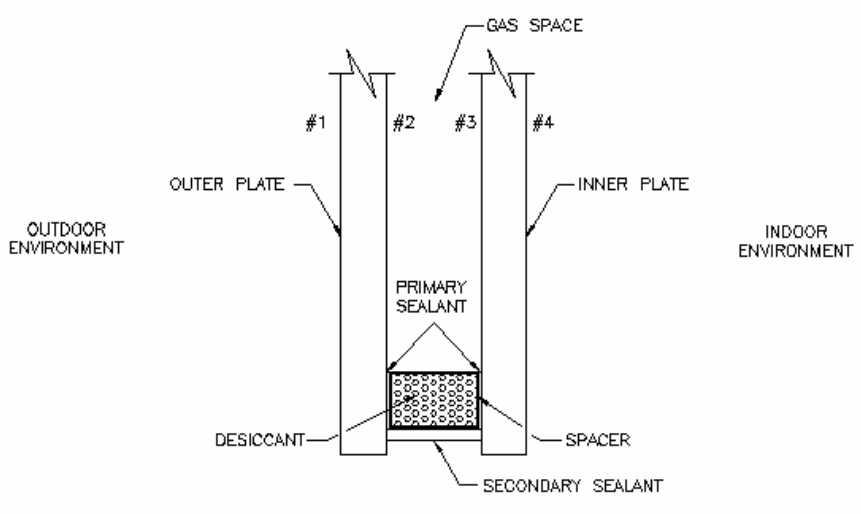

Fig. 3. Primary components of an IG unit

If an IG unit and monolithic glass plate are placed in the same indoor and outdoor environmental conditions, the total energy exchange coefficient for the #1 and #4 surfaces due to conduction, convection, and long wave radiation should reasonably be the same.

Therefore, it is assumed that the total energy exchange coefficients developed for the design of monolithic glass plates can be applied directly to the #1 and #4 surfaces of IG units.

It is desired to develop a single cavity total energy exchange coefficient (CEEC) that can be used to reasonably estimate the total energy exchange between the two IG glass plates through the gas space cavity. This CEEC will be similar to the total energy exchange coefficients used in the development of ASTM E 2431-06 (Beason and Lingnell 2002; ASTM 2006) for surfaces #1 and #4. It is desired that the CEEC accurately model conduction, natural convection, and long wave radiation between the two glass plates. The CEEC will then be used to predict the energy exchange across the gas space cavity based on the linear temperature difference between the two glass plates.

The gas space cavity CEEC will be used to determine the energy transfer between the outer and inner plates through the gas space cavity. Once the energy exchange rates are known, existing monolithic analysis techniques can be modified to accommodate the two glass plates incorporated in IG units, so that the variation of temperature between the center of glass area and perimeter of glass for an IG unit glass plate can be estimated. Then knowing the distribution of temperatures in an IG plate, the associated thermal stresses can be determined using the methodology developed for monolithic glass.

The scope of this thesis is to develop a procedure to determine the gas space CEEC needed for the design of IG units. The CEEC procedure is then coupled with finite element analysis to develop an understanding of the thermal stresses that develop in IG units and how these IG thermal stresses relate to the thermal stresses that develop in monolithic glass plates, given the same set of environmental conditions.

CHAPTER III

LITERATURE REVIEW

Thermal breakage has been one of the leading causes of window failure over the last several years. Thermal breakage in monolithic glass plates typically occurs when perimeter tensile stresses exceed the breaking strength of the glass perimeter. Tensile stresses develop as a result of the center of glass area being warmer than the perimeter of glass. The probability of breakage increases if the perimeter tensile stresses interact with severe edge flaws or impurities causing stress concentrations. This thermal stress situation in glass has long been understood in general terms and an ASTM standard has been developed for the design of monolithic glass plates for thermal stresses induced by solar irradiance (Beason and Lingnell 2002; ASTM 2006). It is believed that a similar procedure can be developed for insulating glass (IG) units if a cavity energy exchange coefficient (CEEC) can be determined for the energy exchange between the plates of an IG unit.

Thermal stresses can be caused by any mechanism that inputs heat into the glass. However, the design of IG units for thermal breakage is primarily associated with short wave solar irradiance (Beason and Lingnell 2002). Thus, this thesis is focused only on short wave solar irradiance as an input mechanism that causes thermal stress.

The most common example that is used to describe a thermal design condition for monolithic glass is the case of cold winter nights. During the night, the center of glass area and the perimeter of glass reach an equilibrium state with the environment. As the sun begins to rise, solar irradiance impinges on the glass and the center of glass area begins to absorb energy. The absorbed energy is transformed into heat and raises the temperature of the center of glass area, which causes the heated area to expand. At the same

time, the perimeter of glass remains at or near the previous night's temperature because it is shielded from direct sunlight, usually through framing, a glazing bead, or a fillet of glazing sealant. Based on this, the perimeter of glass will heat only through conduction from the center of the plate or framing. Therefore, the perimeter of the glass expands at a slower rate than the center of glass area. This situation causes compressive stresses in the center of glass area, and tensile stresses along the perimeter of the glass (Turner 1977, Wright and Barry 1999; Beason and Lingnell 2002), as shown in Fig. 4. If the tensile stresses that develop along the perimeter of the glass exceed the perimeter tensile strength, then breakage will result.

Fig. 4. illustrates the center of glass area, edge of glass, and perimeter of glass. For the typical thermal design situation discussed above, the center of glass area develops compressive stresses while the perimeter of glass develops tensile stresses because the center of glass area is warmer than the perimeter of glass. Heat transfer through the center of glass area is primarily perpendicular to the plane of the plate and for practical purposes can be considered to be a one-dimensional heat transfer process. The edge of glass is the area where the temperature transitions from the center of glass temperature to the perimeter of glass temperature and for practical purposes is generally taken to be a two-dimensional heat transfer process. Finally, the perimeter of glass is the area along the edge where maximum thermal stresses develop (Finlayson et al. 1993).

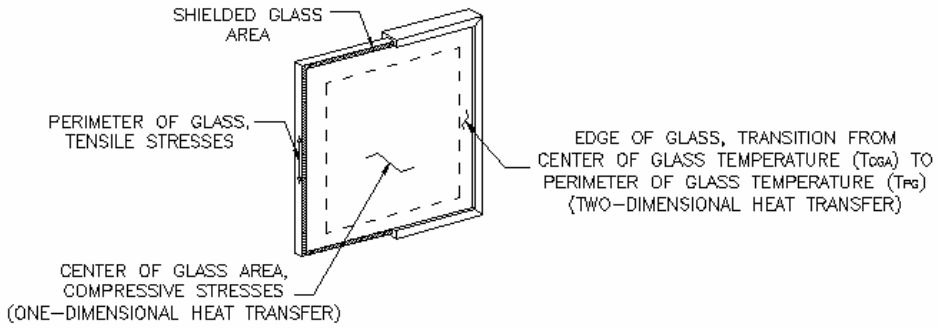

Fig. 4. Illustration of compressive and tensile stresses for monolithic glass plates

It is generally accepted that the thermal stresses that develop due to the above scenario are proportional to the temperature difference between the center of glass area and the perimeter of glass, as given by Eq. (1), (Turner 1977; Wright and Barry 1999; Zhong-wei et al. 1999; Pilkington 2005):

$$\sigma = \alpha_T \, E \, (T_{CGA} - T_{PG}) \tag{1}$$

where σ is the stress along the perimeter of the glass, α_T is the coefficient of thermal expansion, E is Young's modulus, T_{CGA} is the temperature of the center of glass area, and T_{PG} is the perimeter of glass temperature as previously discussed and shown in Fig. 4.

The following section discusses background information on solar irradiance and the fundamental heat transfer mechanisms of conduction, convection, and long wave radiation as applied to energy exchange between monolithic glass plates and the surrounding environment. Next, a discussion of the use of total energy exchange coefficients in the design of monolithic glass plates is presented. This is followed by a discussion of energy exchange between IG units and the surrounding environment. Finally, a discussion on heat transfer through gas space cavities is presented.

Energy Exchange Between Monolithic Glass Plates and the Surrounding Environment

If a monolithic glass plate is taken from a room temperature of 20 ^{o}C and placed in the sun on a hot summer day, the temperature of the glass plate will begin to rise. This rise in temperature is a function of the interaction between the monolithic glass plate and the surrounding environment. Energy exchange between a monolithic glass plate and the surrounding environment can be modeled based on the first law of thermodynamics which states: energy is conserved in a closed system. The monolithic glass plate is considered the closed system. A monolithic glass plate does not consume or generate energy; therefore, the change in internal energy is the difference between the energy that

enters the system and the energy that exits the system. The energy entering the system is in the form of absorbed short wave solar irradiance. This energy is then converted to heat which raises the temperature of the glass plate. The system then exchanges energy with the surrounding environment through the fundamental heat transfer mechanisms of conduction, convection, and long wave radiation (Beason and Lingnell 2002; ASHRAE 2005).

Indoor and outdoor environmental conditions are major factors that affect the variation of temperature of a glass plate with time. The portion of solar irradiance absorbed by the monolithic glass plate is converted to heat which increases the temperature of the glass. The monolithic glass plate then exchanges energy with the outdoor environment through conduction, forced convection, and long wave radiation. At the same time, energy is conducted through the monolithic glass plate and is exchanged with the indoor environment through conduction, natural convection, and long wave radiation. All these factors contribute to the temperature increase of the monolithic glass plate subjected to solar irradiance (Muneer et al. 2000; ASHRAE 2005). The energy exchange between a monolithic glass plate and the surrounding environment can be seen in Fig. 5.

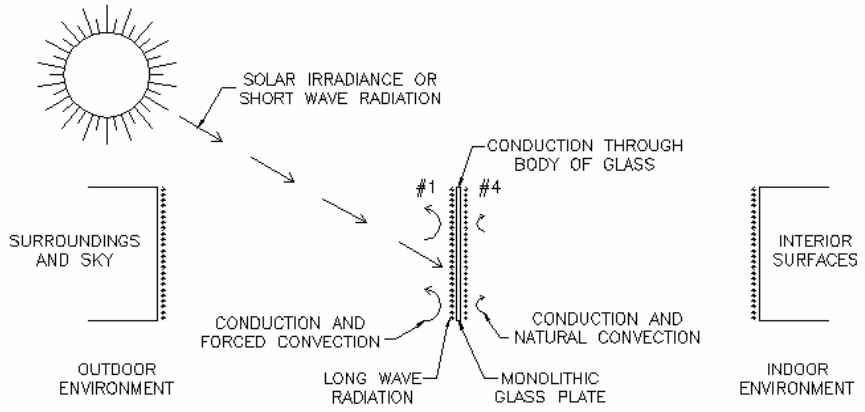

Fig. 5. Illustration of energy exchange between a monolithic glass plate and the indoor/outdoor environment

For thermal analysis of monolithic glass plates presented in ASTM E 2431-06 (Beason and Lingnell 2002; ASTM 2006), the environmental conditions consist of the effective outdoor/indoor temperature and outdoor/indoor total energy exchange coefficients. The effective outdoor temperature is the average temperature of all objects such as the sky, ground, buildings, trees, and other. The effective indoor temperature is the average temperature of all the interior objects such as the walls, floors, ceilings, desks, and other. For practical purposes, the effective outdoor temperature and effective indoor temperature are taken to be the outdoor and indoor air temperatures, respectively (ASHRAE 2005). The total energy exchange coefficients combine the effects of conduction, convection, and long wave radiation into a single constant term. This term is then coupled with the difference between outdoor/indoor temperature and glass plate temperature to calculate the energy exchange between the outdoor/indoor environment and the monolithic glass plate.

Input: Short Wave Radiation/ Solar Irradiance Applied to Monolithic Glass Plates

Solar irradiance is used to describe the amount of short wave electromagnetic radiation that strikes a surface. Solar irradiance varies in wavelength from approximately 0.3 μm to 3μm. Solar irradiance is categorized by wavelengths which include approximately: 5% ultraviolet radiation 0.3 μm < λ < 0.4 μm, 40% visible radiation 0.4 μm < λ < 0.7μm, and 55% near infrared radiation 0.7 μm < λ < 3 μm (Gordon 2001; ASHRAE 2005).

Solar irradiance comes in the form of beam and diffuse short wave electromagnetic radiation. When solar irradiance reaches an object directly without being scattered by the atmosphere it is referred to as beam radiation. If the solar irradiance has been scattered by the atmosphere or reflected from the ground it is referred to as diffuse radiation. The sum of the beam and diffuse radiation acting on a surface is referred to herein as solar irradiance (Duffie and Beckman 1974; ASHRAE 2005).

When solar irradiance strikes a monolithic glass plate: a portion of the solar irradiance is reflected back to the outdoor environment by the glass, another portion of the solar irradiance is transmitted through the glass to the indoor environment, and the remainder of the solar irradiance is absorbed by the glass, as shown in Fig. 6. The portion of solar irradiance that is transmitted, reflected, or absorbed is quantified by the optical properties of the glass, which are typically determined and published by the manufacturer. These optical properties are referred to herein as the solar reflectance (ρ), solar transmittance (τ), and solar absorptance (α). Given any two optical properties, the third property can be calculated using Eq. (2), (Muneer et al. 2000; Gordon 2001; ASHRAE 2005).

$$\alpha + \rho + \tau = 1 \tag{2}$$

The solar absorptance, solar reflectance, and solar transmittance are a function of wavelength and angle of incidence; however, the optical properties do not change significantly with respect to wavelength or when the angle of incidence is less than 40 degrees. Thus, manufacturers typically specify the optical properties as a hemispherical average over the solar spectrum when the angle of incidence is normal to the glass surface (Gordon 2001; ASHRAE 2005).

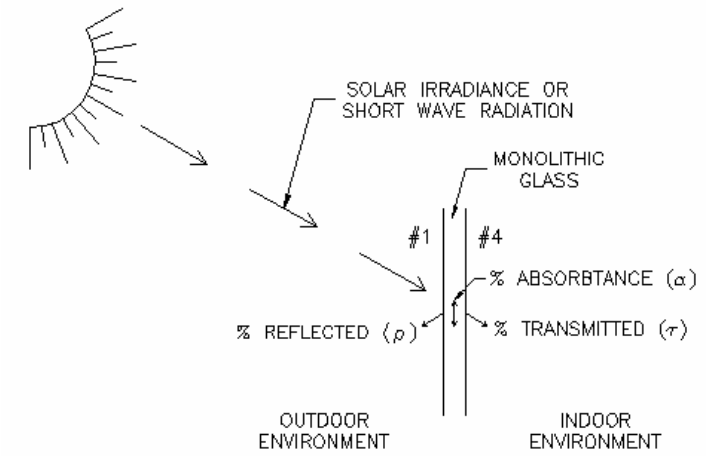

Fig. 6. Reflectance, absorptance, and transmittance of a monolithic glass plate

The absorbed solar irradiance is the input energy that causes a change in glass plate temperature. Thus, energy enters the system through absorbed solar irradiance. The absorbed solar irradiance raises the temperature of the glass plate. Energy is then lost from the plate through a combination of three different mechanisms: conduction, convection, and long wave radiation.

The mechanisms of heat transfer as applied to monolithic glass are discussed next. In addition, there is a final discussion on total energy exchange coefficients that are used for the design of monolithic glass plates.

Conduction

Conduction is used to describe heat flow through a medium such as a solid, liquid, or a gas. As an objects' temperature begins to increase, its' molecular energy increases. This energy is then transferred from higher energy molecules to lower energy molecules through rotational, translational, and/or vibrational energy. Higher molecular energy is associated with higher temperatures; therefore, energy flows from hotter bodies to colder bodies. The rate at which an object conducts heat is quantified by its thermal conductivity (k). Objects range from good conductors that have a high rate of heat transfer (large k), to insulators that have a low rate of heat transfer (small k), (Thomas 1992; Datta 2002).

Fourier's law of conduction is used to calculate one-dimensional steady state heat transfer, as given by Eq. (3):

$$\frac{q}{A} = \frac{k}{L}(T_j - T_k) \tag{3}$$

where q is the conduction energy flow in the transverse direction, A is the area perpendicular to the energy flow, L is the length of flow, the temperatures T_j and T_k are associ

ated with surface j and surface k when a medium is differentially heated. Fourier's law of conduction, as presented in Eq. (3), assumes that the thermal conductivity is constant with respect to temperature, and heat transfer occurs in one direction. For two-dimensional steady state conduction a finite difference or finite element method may be required (Thomas 1992; Datta 2002).

For transient conduction through a medium, an objects' specific heat must be known. The specific heat describes the amount of energy required to raise a unit mass of solid one degree. Therefore, an objects' thermal conductivity describes the ease of heat flow through a material, while the specific heat describes how easily an object will change temperature (Datta 2002).

For monolithic glass plates, conduction takes place through the body of the glass and the air in contact with the glass surface. As previously stated, energy flow through the center of glass area is one-dimensional and energy flow at the edge of glass is two-dimensional. Thus, Eq. (3) can be used for conduction through the center of glass area and a finite difference or finite element method can be utilized for conduction in the edge of glass. Conduction between a monolithic glass plate and air at the glass surface is typically combined with convection in a combined conduction/convection term, which is discussed in the next section.

Convection

Convection is heat transfer from a surface to a fluid based on conduction and fluid motion. Convection is associated with thermal processes that involve liquids or gases. Two types of convection exist: natural convection and forced convection.

The differential equation used to model convection heat transfer involves both conduction and fluid motion. The combination of conduction and fluid motion in the different

tial equation can be quite involved; however, to simplify this differential equation it is frequently assumed that a velocity boundary layer and a temperature boundary layer form between the surface and the bulk fluid during convection (Datta 2002).

As fluid flows over a surface, there exists a distance over which the fluid velocity asymptotically changes from the free stream velocity to zero at the surface. This distance is usually referred to as the velocity boundary layer. For practical applications, the significant effects of the fluid on a surface take place in the velocity boundary layer (Thomas 1992; Datta 2002).

Similar to the velocity boundary layer, a temperature boundary layer forms if there is a temperature difference between the bulk fluid and the surface. The temperature boundary layer is the distance over which the temperature asymptotically changes from the bulk fluid temperature to the surface temperature. For practical applications, the significant effects of the temperature on a surface take place in the temperature boundary layer. As a simplifying assumption, the thermal properties of the fluid can be calculated as the average between the glass surface temperature, T_{GL}, and the temperature of the environment, T_{ENV}. This average temperature is referred to herein as the Film_Temperature and is given by Eq. (4), (Thomas 1992; Datta 2002).

$$\text{Film\_Temperature} = \frac{T_{GL} + T_{ENV}}{2} \tag{4}$$

Based on the simplifying assumptions of velocity and temperature boundary layers, a convection coefficient, which combines the effects of conduction and convection, can be determined. The convection coefficient, $h_{CONVECTION}$, given by Eq. (5) is expressed in terms of a dimensionless parameter known as the Nusselt number (Nu):

$$h_{CONVECTION} = \frac{Nu\ k_{FLUID}}{L} \tag{5}$$

where L is the characteristic length of the surface and k_{FLUID} is the thermal conductivity of the fluid. For flat plates, the characteristic length (L) is the distance across the surface parallel to the fluid flow. The minimum Nusselt number associated with Eq. (5) is 1.0, which corresponds to pure conduction.

Natural convection takes place when a surface and the surrounding fluid reside at different temperatures. As the temperature of the surface increases, the gas touching the plate heats through conduction, the heated gas then expands and rises along the surface of the plate due to buoyant forces caused by a decrease in density. As the heated gas leaves its original location, adjacent gas moves in to fill the void creating a current. The gas that fills the void then begins to heat and the process is repeated, creating natural convection (Thomas 1992; Datta 2002).

For natural convection on a heated vertical surface, the Nusselt number is expressed in terms of the Rayleigh number (Ra), and Prandtl number (Pr) as given by Eqs. (6), (Datta 2002).

$$\mathrm{Nu} = \left[0.825 + \frac{0.387\mathrm{Ra}^{\frac{1}{6}}}{\left(1 + \left(\frac{0.492}{\mathrm{Pr}} \right)^{\frac{9}{16}} \right)^{\frac{8}{27}}} \right]^2 \tag{6}$$

The Rayleigh number, as given by Eq. (7), is the product of the Prandtl number and the Grashof number (Gr). The prandtl number, as given by Eq. (8), is the ratio of viscous effect to thermal diffusion effect and the Grashof number, as given by Eq. (9), is the ratio of buoyancy force to viscous force:

$$Ra = Gr\ Pr \tag{7}$$

$$Gr = \frac{\beta\, g\, L^3\, (T_{ENV} - T_{GL})}{\upsilon^2} \tag{8}$$

$$Pr = \frac{\upsilon}{\alpha_D} \tag{9}$$

where β is 1/Film_Temperature for ideal gases, g is the local gravitational constant for the surface of the earth, L is the characteristic length, T_{GL} is the temperature of the glass surface, T_{ENV} is the temperature of the environment, υ is the kinematic viscosity of the fluid, and α_D is the thermal diffusivity of the fluid (Datta 2002).

Forced convection occurs when a fluid is forced across a surface such as wind blowing across the face of a building. Heat transfer due to forced convection occurs at a higher rate than natural convection because the fluid is pushed by external forces rather than driven by buoyant forces. The fluid motion can range from laminar flow to turbulent flow and is characterized by the Reynolds number (Re). The Reynolds number is the ratio of inertia force to viscous force, as given by Eq. (10):

$$Re = \frac{u\ x\ \rho_m}{\mu} \tag{10}$$

where u is the free stream velocity, x is distance from the leading edge of the plate parallel to fluid flow, ρ_m is the density of the fluid, and μ is the viscosity of the fluid (Datta 2002). Laminar flow, $Re < 2 \times 10^5$, is associated with orderly flow of a fluid, while turbulent flow, $Re > 3 \times 10^6$, is associated with chaotic flow of a fluid that generates mixing and therefore has a higher rate of heat transfer. The transition region, $2 \times 10^5 \leq Re \leq 3 \times 10^6$, is the region over which the flow transitions from laminar to turbulent flow (Thomas 1992; Datta 2002).

For flat plate forced convection, Eqs. (11) and (12) can be used to obtain the Nusselt number for laminar and turbulent flow (Datta 2002).

$$Nu = 0.664\ Re^{\frac{1}{2}}\ Pr^{\frac{1}{3}} \quad \text{for laminar } (Re < 2 \times 10^5) \tag{11}$$

$$Nu = 0.0360\ Re^{\frac{4}{5}}\ Pr^{\frac{1}{3}} \quad \text{for turbulent } (Re < 3 \times 10^6) \tag{12}$$

For convection heat transfer between a monolithic glass plate and the surrounding environment, it is typically assumed that forced convection takes place on the outdoor (#1) surface and natural convection takes place on the indoor (#4) surface. The Nusselt numbers described by Eqs. (6) through (12) can then be used to calculate a convection coefficient, $h_{CONVECTION}$. The energy transfer due to the combined effects of conduction and convection for a particular situation can then be calculated by Newton's law of cooling, Eq. (13).

$$\frac{q}{A} = h_{CONVECTION}\ (T_{ENV} - T_{GL}) \tag{13}$$

Where q is the convective energy flow and all other terms in Eq. (13) are as previously defined.

Long Wave Radiation

All matter that resides at a temperature above absolute zero emits electromagnetic radiation (Datta 2002; ASHRAE 2005). Radiation associated with objects at or near room temperature have wavelengths ranging from approximately 3 μm to 50 μm (Gordon 2001; ASHRAE 2005) and is referred to herein as long wave radiation. The net energy exchange by long wave radiation between two objects is based on their temperature difference as given by Eq. (14):

$$\frac{q}{A} = \sigma_{SB}\ \varepsilon\ (T_{ENV}^4 - T_{GL}^4) \tag{14}$$

where q is the long wave radiation energy flow in the transverse direction, A is the area perpendicular to the transverse direction, σ_{SB} is the Steffan-Boltzmann constant, ε is the emissivity of the radiating surface, T_{GL} is the absolute glass surface temperature, and T_{ENV} is the absolute environment temperature. This energy exchange is unique in the fact that it does not require a medium, such as air, for the energy exchange to take place. A temperature difference is all that is required (Thomas 1992; Datta 2002).

The amount of long wave radiation that is radiated by an object is quantified by the object's emissivity. A blackbody is used to describe an object that emits the maximum amount of theoretical radiation possible, emissivity equal to 1. An object's emissivity is the ratio of the objects emissive power to the emissive power of a black body of the same temperature. The emissivity of an object varies as a function of wavelength; however, as a simplifying assumption, it is generally assumed that the emissivity of an object is an average over all wavelengths or a hemispherical average (Datta 2002; ASHRAE 2005). This is the case because all of the sources of thermal radiation are diffusely emitting (Rubin 1982).

Long wave radiation and solar irradiance (short wave radiation) are both forms of radiation. However, they are classified differently because of the wavelengths associated with each type of radiation. As a general rule, objects below 1200 ^{o}C will emit long wave radiation and objects above 1200 ^{o}C will emit short wave radiation (ASHRAE 2005). Typical monolithic glass plate temperatures will be significantly lower than 1200 ^{o}C, thus monolithic glass plates emit long wave radiation. Based on this, there is not an appreciable overlap between the wavelengths associated with solar irradiance and long wave radiation, thus two independent analyses can be utilized. One analysis is used for solar irradiance and one analysis is used for long wave radiation, as previously discussed (Gordon 2001; ASHRAE 2005).

As previously discussed, energy enters the system through absorbed solar irradiance which raises the temperature of the glass. Energy then exits the system through conduction, convection, and long wave radiation. A portion of the input solar irradiance (short wave radiation) will be reflected, transmitted, or absorbed by a monolithic glass plate; however, this is not the case for long wave radiation. Window glass will not transmit long wave radiation. Thus, all of the long wave radiation is either reflected or absorbed (Thomas 1992; ASHRAE 2005).

Long wave radiation energy exchange takes place between a monolithic glass plate surface and the surrounding outdoor/indoor environment. In addition, it can be assumed that air is a non-participating gas and has no effect on input solar irradiance or long wave radiation (Muneer et al. 1997; Ismail and Henriquez 2005).

Total Energy Exchange Coefficients

The nonlinear nature of the energy exchange due to conduction, convection, and long wave radiation between a monolithic glass plate and the surrounding environment greatly complicates the thermal analysis. For design purposes a single total energy exchange coefficient that combines the effects of conduction/convection, and long wave radiation is desired. The use of a single total energy exchange coefficient simplifies the numerical analysis by eliminating the need for iteration (Gordon 2001).

As previously discussed, the Nusselt number can be calculated by Eq. (6) for natural convection and Eqs. (11) or (12) for forced convection. The calculated Nusselt number can then be input into Eq. (15) to determine an effective convection energy exchange coefficient, $h_{CONVECTION}$.

$$h_{CONVECTION} = \frac{Nu\ k}{L} \tag{15}$$

By equating Newton's law of cooling, Eq. (13), and the radiation energy exchange, Eq. (14), a radiation energy exchange coefficient, $h_{RADIATION}$, can be determined, as given by Eq. (16), (Gordon 2001):

$$h_{RADIATION} = \sigma_{SB}\, \varepsilon\, (T_{GL} + T_{ENV})\, (T_{GL}^2 + T_{ENV}^2) \tag{16}$$

where all of the variables in Eqs. (15) and (16) are as previously defined.

Eq. (16) results in an effective radiation energy exchange coefficient that can be combined with the effective convection coefficient, Eq. (15), to determine the total energy exchange coefficient, h_{TOTAL}, as given by Eq. (17), (Gordon 2001).

$$h_{TOTAL} = h_{CONVECTION} + h_{RADIATION} \tag{17}$$

For outdoor environmental conditions, the total energy exchange coefficient, $h_{TOTAL\_OUTDOOR}$, combines the effect of conduction, forced convection, and long wave radiation loss to the surrounding environment. For indoor environmental conditions, the total energy exchange coefficient, h_{TOTAL_INDOOR}, combines the effect of conduction, natural convection, and long wave radiation loss to the indoor environment (Gordon 2001; ASHRAE 2005).

The total energy exchange coefficient, h_{TOTAL}, is then coupled with Newton's law of cooling, Eq. (18), and used to determine the total energy exchange between a monolithic glass plate surface and the surrounding environment:

$$\frac{q}{A} = h_{TOTAL}\, (T_{ENV} - T_{GL}) \tag{18}$$

where q is the combined energy exchange from conduction, convection, and long wave radiation, T_{ENV} is the temperature of the outdoor/indoor environment, and T_{GL} is the temperature of the glass surface.

Conservation of energy principles can then be used to quantify the amount of energy exchanged between a monolithic glass plate and the surrounding environment. The monolithic glass plate is considered to be the closed system. Energy enters the system through absorbed solar irradiance, and energy exits the system through the outdoor and indoor total energy exchange coefficients (Beason and Lingnell 2002). The closed system is illustrated in Fig. 7.

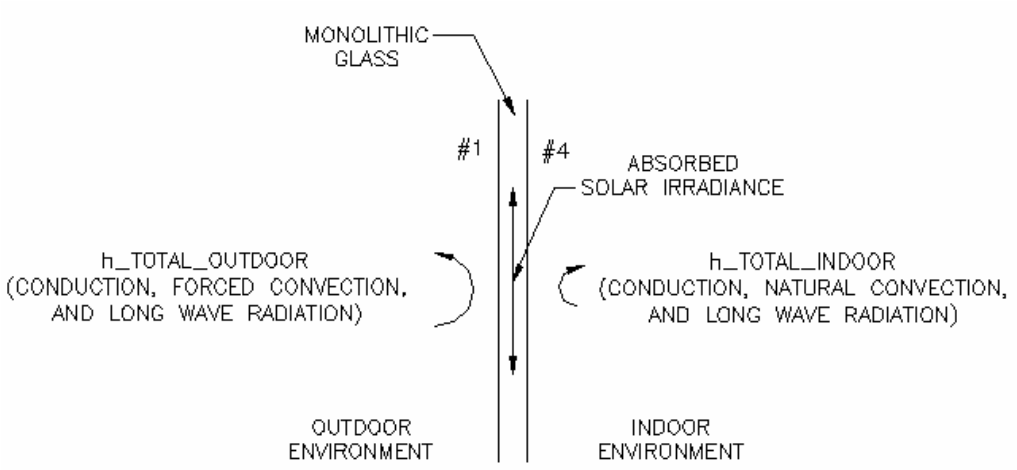

Fig. 7. Closed system for monolithic glass plate using total energy exchange coefficients

A design procedure to determine the probability of failure for monolithic glass subjected to solar irradiance has been presented in ASTM E 2431-06. This procedure assumes that a monolithic glass plate exchanges energy with the outdoor and indoor environment based on the total energy exchange coefficients of 13.55 W/(m^2 K) and 8.04 W/(m^2 K), respectively (Beason and Lingnell 2002; ASTM 2006).

The total indoor energy exchange coefficient of 8.04 W/(m^2 K), as presented in ASHRAE (2005) and recommended by Beason and Lingnell (2002), is within 5% of the value of 8.3 W/(m^2 K) recommended by Muneer (et al. 2000) for typical indoor energy exchange conditions. Thus, a value of 8.04 W/(m^2 K) is believed to be representative of typical indoor energy exchange conditions for monolithic glass plates that do not have indoor energy traps such as Venetian blinds or curtains.

The outdoor total energy exchange coefficient of 13.55 W/(m^2 K), recommended by Beason and Lingnell (2002), is within 10% of the value of 12.5 W/(m^2 K) recommended by Muneer (et al. 2000) for a sheltered condition. Based on this, it is believed that this coefficient is representative of a relatively sheltered condition where there will be minimal energy exchange between a monolithic glass plate and the surrounding environment. This sheltered condition results in smaller energy exchange with the outdoor environment than would be the case if the window were subjected to the direct effects of the wind. Thus, use of the coefficient for sheltered conditions leads to higher glass plate temperatures.

If a monolithic glass plate and an IG unit are placed in the same environmental conditions, the total energy exchange coefficients on the indoor and outdoor surface would be the same. Therefore, it is believed that the total energy exchange coefficients used in the development of ASTM E 2431-06 can be applied directly to the design of IG units. In addition, a total energy exchange coefficient that combines the effects of conduction, natural convection, and long wave radiation through IG gas spaces is desired for the design of IG units. A discussion of the energy exchange between IG units and the surrounding environment is presented next.

Energy Exchange Between an IG Unit and the Surrounding Environment

If an IG unit is taken from room temperature of 20 ^{o}C and placed in the sun on a hot summer day, the temperature of the inner and outer plate would begin to rise. This rise in temperature is a function of the interaction between the IG unit and the surrounding environment. The heat transfer mechanisms of conduction, convection, and long wave radiation discussed previously for monolithic glass plates apply directly to IG units.

Similar to monolithic glass plates, the conservation of energy principles can be used to determine the amount of energy that is exchanged between an IG unit and the surrounding environment. Each plate of an IG unit can be considered a closed system and is represented by a control volume. Energy enters the system through absorbed solar irradiance. The solar irradiance is proportioned to the outer and inner plate by the ray tracing procedure discussed in the following section. This energy is converted to heat which changes the temperature of the outer and inner plate. Energy is then exchanged through the fundamental heat transfer mechanisms of conduction, convection, and long wave radiation: with the outdoor environment, across the gas space cavity, and with the indoor environment, as shown in Fig. 8.

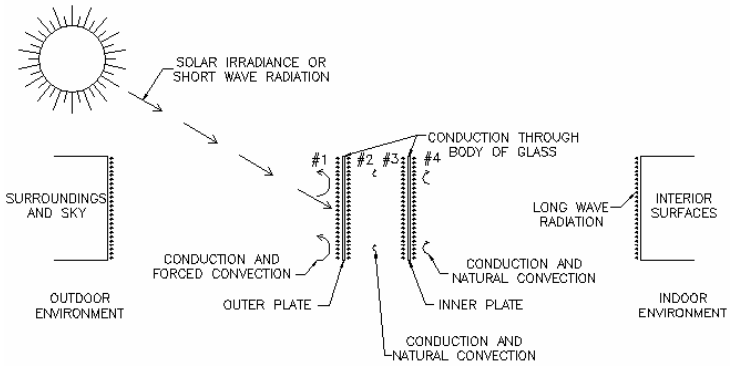

Fig. 8. Illustration of energy exchange between an IG unit and the indoor/outdoor environment

Input: Solar Irradiance/Short Wave Radiation as Applied to IG Units

A process known as ray tracing is used to determine the amount of solar irradiance that is absorbed, transmitted, and reflected from the inner and outer plates of an IG unit. As shown in Fig. 9, when solar irradiance strikes an IG unit: a portion of the solar irradiance is reflected back to the outdoor environment by the glass, a portion of the solar irradiance is transmitted through the glass to the inner plate and the remainder of the solar irradiance is absorbed by the glass. The solar irradiance that is transmitted to the inner plate is either absorbed by the inner plate, reflected to the outer plate, or transmitted to the indoor environment based on the properties of the inner plate. The inner-reflectance continues between the outer and inner plate until all of the energy is absorbed or transmitted (Wijeysundera 1975; Gordon 2001; ASHRAE 2005).

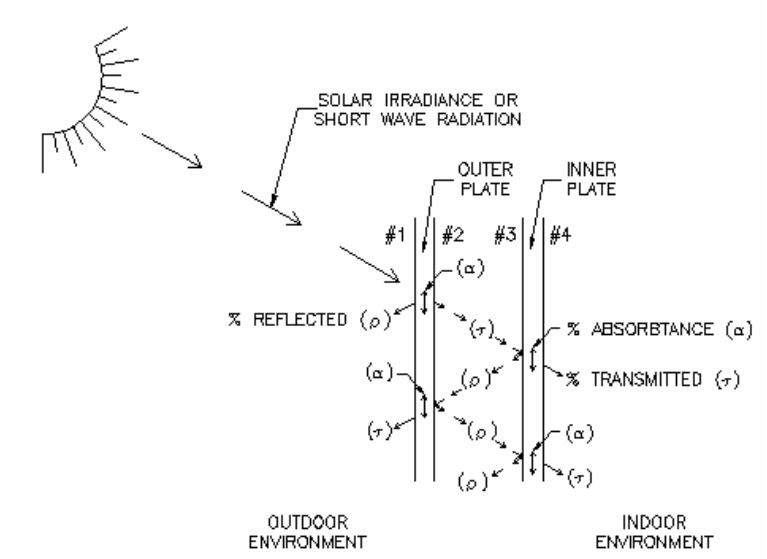

Fig. 9. Ray tracing

Once the amount of energy has been proportioned to the outer and inner plates by ray tracing, an energy balance can be written for each plate of an IG unit and the surrounding environment to determine the variation of temperature for a given set of conditions.

Unlike monolithic glass plates, the plates of an IG unit are separated by a gas space cavity. The gas space cavity incorporates conduction, natural convection, and long wave radiation; which is discussed in the next section.

Energy Exchange Across Gas Space Cavities

IG units incorporate energy exchange between the outer and inner plate through the gas space cavity. This energy exchange is controlled by conduction, natural convection, long wave radiation. The radiation energy exchange through the gas space cavity is discussed next, followed by conduction and natural convection energy exchange.

IG units consist of two glass plates separated by a gas space which can be modeled as two parallel plates. The radiation exchange between parallel plates can be calculated using Eq. (19) coupled with an effective emissivity. The effective emissivity takes into account the emissivity of the #2 and #3 surfaces, and is calculated by Eq. (20), (ASHRAE 2005):

$$\frac{q}{A} = \sigma_{SB}\, \varepsilon_{EFFECTIVE}\, (T_2^4 - T_3^4) \tag{19}$$

$$\varepsilon_{EFFECTIVE} = \frac{1}{\frac{1}{\varepsilon_2} + \frac{1}{\varepsilon_3} - 1} \tag{20}$$

where q is the radiation energy flow in the transverse direction through the gas space cavity, T_2 is the absolute temperature of surface #2, T_3 is the absolute temperature of sur-

face #3, $\varepsilon_{EFFECITIVE}$ is the effective emissivity between parallel plates, ε_2 is the emissivity of surface #2, and ε_3 is the emissivity of surface #3.

In addition to radiation, energy exchange from conduction and natural convection also occurs. Many studies have been conducted to mathematically model the energy transfer across gas space cavities (Elder 1965; El Sherbiny et al. 1982; Han and Muneer 1996; Wright 1996). Wright (1996), presents a correlation specifically for determining the center of glass convective energy transfer for windows and is discussed below. The correlation is independent of aspect ratio and can be used in applications involving high Rayleigh numbers.

Conduction and natural convection through gas space cavities can range from pure conduction to turbulent natural convection based on the temperature difference between the plates and the orientation of the IG unit. For vertical cavities at lower temperature differences, the energy exchange is primarily through conduction, while at higher temperature differences, the energy exchange is primarily through natural convection. The conduction and natural convection energy exchange through gas space cavities is computed by Eq. (21) where a convection coefficient is calculated based on Eq. (22) and the Nusselt number is a function of the Rayleigh number, as given in Eqs. (23) through (25). Eqs. (23) through (25) are believed to be the most widely accepted formulation for determining the Nusselt number for vertical gas space cavities (Wright 1996).

$$\frac{q}{A} = h_{CONVECTION}\,(T_2 - T_3) \tag{21}$$

$$h_{CONVECTION} = \frac{Nu\ k_{FLUID}}{L} \tag{22}$$

$$Nu = 0.0673838\ \ Ra^{\frac{1}{3}} \qquad Ra > 5 \times 10^4 \tag{23}$$

$$Nu = 0.028154\ \ Ra^{0.4134} \qquad 1 \times 10^4 < Ra \le 5 \times 10^4 \tag{24}$$

$$Nu = 1 + 1.75967 \times 10^{-10}\ \ Ra^{2.2984755} \qquad Ra \le 1 \times 10^4 \tag{25}$$

Eqs. (19) through (25) can be used to accurately model the energy exchange through the gas space cavity; however, the effects of conduction, natural convection, and long wave radiation combine in a nonlinear fashion. The nonlinear nature of the gas space energy exchange complicates the numerical analyses required to determine the temperature distribution needed to estimate thermal stresses. For design purposes, a total cavity energy exchange coefficient is desired to proportion the amount of energy exchanged between the outer and inner plate of an IG unit. The desired design system can be seen in Fig. 10. Chapter IV is dedicated to the development of a numerical propagation procedure to determine the total cavity energy exchange coefficient, CEEC.

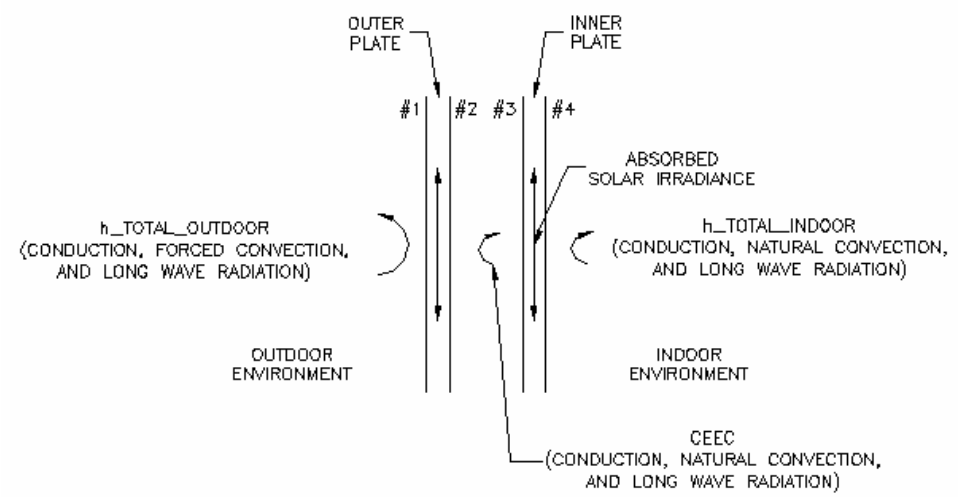

Fig. 10. Design system for IG units using total energy exchange coefficients

CHAPTER IV

NUMERICAL PROPAGATION PROCEDURE

Chapter IV is dedicated to the development of a single constant term to represent the energy exchange due to conduction, natural convection, and long wave radiation between the center of glass area of the outer/inner plate of an insulating glass (IG) unit. This total energy exchange coefficient is referred to herein as the cavity energy exchange coefficient (CEEC). The use of the CEEC value greatly simplifies the thermal analysis of IG units by eliminating the nonlinear iterative procedures currently required to predict temperatures of windows that incorporate gas space cavities.

The next section presents the generic numerical propagation procedure. This is followed by a section that describes how the numerical propagation procedure is used to determine the center of glass equilibrium temperature with the surrounding environment for an IG unit. This is followed by a section that describes how the numerical propagation procedure is used to determine the transient center of glass temperature for an IG unit. Finally, a section that describes the calculation of the CEEC value for an IG unit is presented.

Nonlinear Numerical Propagation Procedure

The purpose of this section is to present a numerical propagation procedure that can be used to determine the CEEC value for an IG unit subjected to a defined set of environmental conditions. The numerical propagation procedure results in the outer/inner glass plate temperatures as a function of time. This problem is a classic conservation of energy problem, where the glass plates of the IG unit receive input through solar irradiance and exchange energy with each other and the surrounding environment. For this analy-

sis, it is necessary to know the energy exchange rate between the outer glass plate and the outdoor environment, the inner glass plate and the indoor environment, and the energy exchange through the gas space cavity. In addition, it is necessary to be able to estimate the amount of solar irradiance absorbed by the outer and inner glass plates when the IG unit is subjected to a defined level of solar irradiance.

For the research presented herein, it was assumed that the outer plate exchanges energy with the outdoor environment based on a total energy exchange coefficient of 13.55 $W/(m^2 K)$ as recommended by Beason and Lingnell (2002). Based upon previous discussions, it is believed that this coefficient is representative of a relatively sheltered condition.

In addition, it was assumed that the inner plate exchanges energy with the indoor environment based on a total energy exchange coefficient of 8.04 $W/(m^2 K)$ as presented in ASHRAE (2005) and recommended by Beason and Lingnell (2002). This value is believed to be representative of typical indoor energy exchange conditions for IG units that do not have indoor energy traps, such as Venetian blinds or curtains.

The energy exchange rate, q/A, through the gas space cavity due to natural convection was calculated using Eq (26). The nonlinear energy exchange rate, q/A for radiation, was calculated using Eq. (27).

$$\frac{q}{A} = h_{CONVECTION} (T_2 - T_3) \tag{26}$$

$$\frac{q}{A} = \sigma_{SB} \varepsilon_{EFFECTIVE} (T_2^4 - T_3^4) \tag{27}$$

All of the terms in Eqs. (26) and (27) are as previously defined.

Given an assumed level of solar irradiance, the outer and inner plates of an IG unit absorb energy based on the optical properties of surfaces #1 through #4. The ray tracing technique, described in Chapter III, was used to determine the portions of solar irradiance absorbed by the outer and inner plates. The fraction of solar irradiance absorbed in the outer and inner plates determined by the ray tracing procedure will be referred to as "Absorptance_Outer" and "Absorptance_Inner", respectively. The absorbed solar irradiances were assumed to be absorbed evenly at all points through the thickness of the glass, over a given time step (Wright 1998; Powles et al. 2002).

The numerical propagation procedure uses the net energy exchange between a plate of an IG unit and the surrounding environment to determine the change in temperature for a given time interval. Based on the outdoor and indoor total energy exchange coefficients, the nonlinear cavity energy exchange from convection and radiation, and the outer/inner plate solar absorptance described above, it is possible to calculate a net energy flux for the outer/inner glass plate of an IG unit over a specified time increment. This value is presented as a net energy flux per unit area. Therefore, a control volume that represents a closed system was defined as a unit area of glass with a thickness of, t_{GL}. Thus, the magnitude of the control volume is equal to the thickness of the glass, t_{GL}. Figs. 11 and 12 present control volumes for the outer and inner glass plates, respectively.

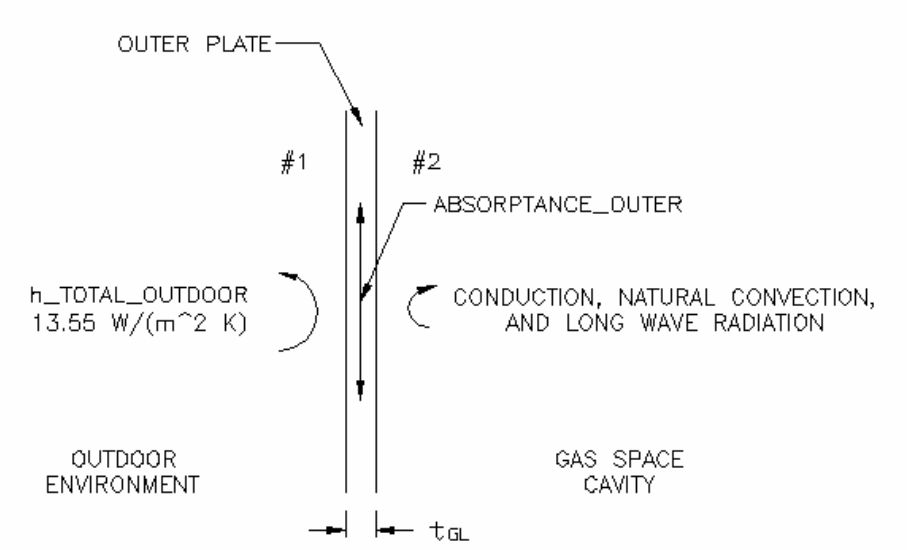

Fig. 11. Outer plate IG unit control volume

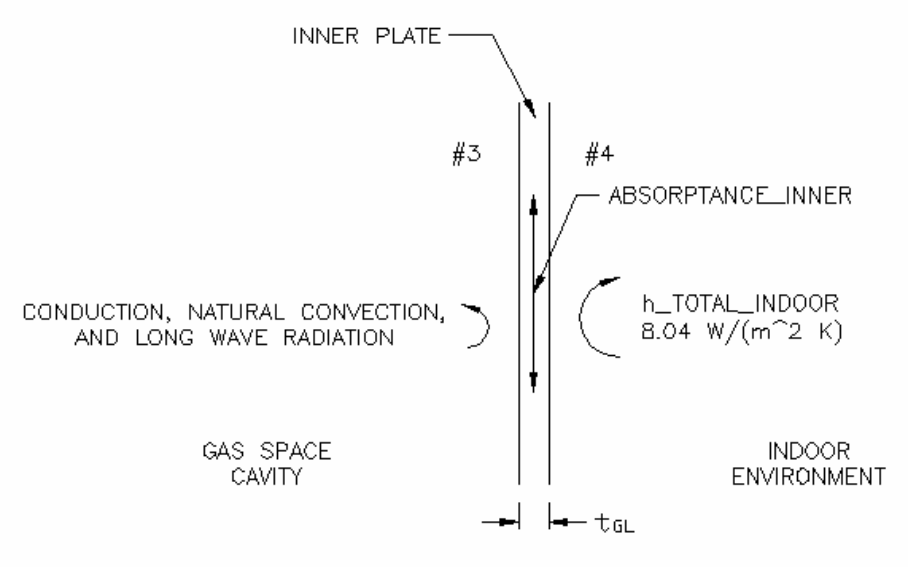

Fig. 12. Inner plate IG unit control volume

The sum of all the energy entering and leaving the plate of an IG unit, as shown in Figs. 11 and 12, is used to determine the net energy flux per unit area, as described by Eqs. (28) and (29):

$$q_{NET\_OUTER} = h_{TOTAL\_OUTDOOR}\,(T_{OUTDOOR}-T_1) + h_{CONVECTION}\,(T_2-T_3) + \sigma_{SB}\,\varepsilon_{EFFECTIVE}(T_2^4 - T_3^4) + Absorptance\_Outer \quad (28)$$

$$q_{NET\_INNER} = h_{TOTAL\_INDOOR}\,(T_{INDOOR}-T_4) + h_{CONVECTION}\,(T_3-T_2) + \sigma_{SB}\,\varepsilon_{EFFECTIVE}(T_3^4 - T_2^4) + Absorptance\_Inner \quad (29)$$

where "q_{NET_OUTER}" is the net energy flux per unit area of the outer plate, "$h_{TOTAL\_OUTDOOR}$" is 13.55 W/(m^2 K), "Absorptance_Outer" is the solar irradiance absorbed by the outer plate, "q_{NET_INNER}" is the net energy flux per unit area of the inner plate, "h_{TOTAL_INDOOR}" is 8.04 W/(m^2 K), "Absorptance_Inner" is the solar irradiance absorbed by the inner plate, "$T_{OUTDOOR}$" is the outdoor temperature, "T_{INDOOR}" is the indoor temperature, T_1 is the temperature of surface #1, T_2 is the temperature of surface #2, T_3 is the temperature of surface #3, and T_4 is the temperature of surface #4. It is generally assumed that the conductance through the glass plate can be neglected which means that for practical purposes $T_1 = T_2$ and $T_3 = T_4$ (Rubin 1982; Pilette and Taylor 1988; Gordon 2001).

If the net energy flux is positive, the glass plate gets warmer over the time interval and if the net energy flux is negative, the glass plate gets cooler over the time interval. The change in temperature ΔT is calculated based on the mass of the control volume, $\rho_m * t_{GL} * 1$ (unit area), and the specific heat of glass as shown in Eq. (30):

$$\Delta T = \frac{q_{NET}\,\Delta t}{1 * \rho_m * t_{GL} * C_P} \quad (30)$$

where ΔT is the change in temperature over the time interval, q_{NET} is the net energy flux per unit area exchanged between an IG control volume and the surrounding environment during the time interval, Δt is the time step, 1 implies unit area, ρ_m is the density of glass, t_{GL} is the thickness of the glass, and C_P is the specific heat of the glass.

Then the new temperature of the control volume, T_{i+1}, at the end of the time interval is found by simply adding the change in temperature, ΔT, to the original temperature, $T_{i,}$ as given by Eq. (31).

$$T_{i+1} = T_i + \Delta T \tag{31}$$

The numerical propagation is begun by assuming an initial set of temperatures and inputs. Then, Eqs. (30) and (31) are used to calculate the temperature at the end of the time interval. Then the process is repeated until the desired output is achieved with the result being the variation of inner and outer plate temperatures as a function of time.

The typical thermal stress situation involves an IG unit that is at equilibrium with its surroundings when it is suddenly exposed to solar irradiance corresponding with sunrise. The thermal stresses that develop in this situation are a function of the temperature differences between the center of glass area and the perimeter of glass. To properly analyze this situation, it is first necessary to establish the initial or equilibrium temperatures of the center of glass area for the outer and inner plates. These initial equilibrium temperatures are then used as a starting point to establish the transient temperatures when the IG unit is suddenly exposed to solar irradiance corresponding to sunrise.

To accomplish this, two different numerical propagation procedures are needed. One to predict the equilibrium center of glass temperatures as a function of the assumed indoor and outdoor temperatures without solar irradiance. This procedure will be referred to as the equilibrium numerical propagation procedure (ENPP). The second procedure is used to predict the variation of the center of glass temperatures when the IG unit is suddenly exposed to solar irradiance. This procedure will be referred to as the numerical propagation procedure with solar absorptance (NPPSA).

Calculation of Cavity Energy Exchange Coefficient (CEEC) Using Nonlinear Least Squares Regression

The numerical propagation procedure discussed in the above section employs Eqs. (28) through (31), coupled with the nonlinear cavity energy exchange, to determine the variation of temperature of the outer and inner glass plates of an IG unit as a function of time. The problem with this procedure is that it is complicated by the use of the nonlinear cavity energy exchange caused by the radiation model presented in Eq. (27).

To circumvent this problem, a constant cavity energy exchange coefficient, CEEC, that can be used to accurately represent the effects of the nonlinear cavity energy exchange is introduced. This method will be referred to as the CEEC procedure. Based on this, the net energy flux calculated in Eqs. (28) and (29) can be rewritten in the form of Eqs. (32) and (33), where the nonlinear energy exchange is replaced by an assumed constant cavity energy exchange coefficient, CEEC. A similar numerical propagation procedure can then be exercised using Eqs. (32) and (33) to determine the variation of temperature for a given IG unit and an assumed CEEC value.

$$q_{NET\_OUTER} = h_{TOTAL\_OUTDOOR}\,(T_{OUTDOOR}-T_1) + CEEC\,(T_2-T_3) + Absorptance\_Outer \quad (32)$$

$$q_{NET\_INNER} = h_{TOTAL\_INDOOR}\,(T_{INDOOR}-T_4) + CEEC\,(T_3-T_2) + Absorptance\_Inner \quad (33)$$

Then, the challenge is to select the best CEEC value that most closely represents the results generated using the nonlinear NPPSA procedure. Nonlinear least squares regression techniques provide one way to estimate the best CEEC value for a given set of conditions. In this procedure, the transient temperature results, "T_{OUTER_i}" and "T_{INNER_i}" from the nonlinear NPPSA presented in the above section are assumed to be the true temperature values as a function of time. The transient temperature results from the linear NPPSA CEEC procedure are used to provide hypothesized temperature values, "$T_{HAT\_OUTER\_i}$" and "$T_{HAT\_INNER\_i}$" , as a function of time. In this case, the best value of CEEC is the only unknown parameter in the hypothesized relationship. Then, the total

error sum of squares, P, associated with the use of a particular value of CEEC can be expressed in the form of Eq. (34).

$$P = \Sigma\left((T_{OUTER\_i} - T_{HAT\_OUTER\_i})^2 + (T_{INNER\_i} - T_{HAT\_INNER\_i})^2\right) \quad (34)$$

Using the well know principles of nonlinear least squares regression, the best value for CEEC for a particular situation is the value that minimizes the total sum of squares, P (Kennedy 1976). One way to accomplish the minimization of P is through the use of minimization techniques incorporated in recent versions of EXCEL. This is done using the EXCEL solver and by setting the total sum of the squares, P, to a minimum by selecting the best value of CEEC.

Practical Application

As an example of the use of the nonlinear numerical propagation procedure, it was assumed that the IG unit consists of two 6 mm, clear glass plates with a 12 mm air space. For this example, the IG unit was subjected to a constant outdoor temperature of 50 ^{o}C, a constant indoor temperature of 20 ^{o}C, a constant outdoor total energy exchange coefficient of 13.55 W/(m^2 K), and a constant indoor total energy exchange coefficient of 8.04 W/(m^2 K). Further, it was assumed that this IG unit is subjected to a solar irradiance of 750 W/m^2.

Various time increments were used in the following analyses to determine the minimum required time step. It was found in this effort that a time step of 15 seconds comfortably works for all of the situations examined. For purposes of the analysis reported herein, the time step was taken to be 15 seconds, the density of glass was taken to be 2511.9 kg/m^3, the specific heat of glass was taken to be 838.3 J/(kg K), the thermal diffusivity of air was taken to be 2.074 x 10^{-5} m^2/s, and the kinematic viscosity of air was taken to be 1.516 x 10^{-5} kg/(m s). Wright (1996), Muneer (1997), Manz (2003), and Gustavsen

(2005) state that all thermophysical properties for air can be taken as constant except for the properties used in the calculation of the Grashof number. For the purposes of this research it was determined that the natural convection calculated from variable gas properties and from constant gas properties resulted in a percent error of less than 5 percent. This level of error was deemed acceptable; therefore, all gas properties were held constant to simplify the analysis.

The first step in the analysis process was to determine the equilibrium temperatures for the center of glass area using the ENPP. It was found that under the prescribed conditions, the center of glass area of the outdoor plate reached an equilibrium temperature of 43.5 ^{o}C and the center of glass area of the indoor plate reached an equilibrium temperature of 30.9 ^{o}C.

The next step was to determine the variation of temperature when the example IG unit was suddenly exposed to solar irradiance, using the NPPSA. The ray tracing procedure was used to determine the amount of energy absorbed by the outer and inner IG plates given the assumed solar irradiance of 750 W/m^2. The outer and inner plates of the example IG unit have an absorptance of 0.1436, reflectance of 0.07086, and transmittance of 0.7855. Figs. 13 and 14 show step by step calculations for determining the total absorptance for the first pass of the ray tracing procedure of the outer and inner plates of the example IG unit, respectively.

In Figs. 13 and 14: “SOLAR INPUT 1, OUTER” is the initial solar irradiance striking the outer plate for pass 1, “ABSORPTANCE 1, OUTER” is the energy absorbed by the outer plate for pass 1, “REFLECTANCE 1, OUTER” is the energy reflected by the outer plate for pass 1, “TRANSMITTANCE 1, OUTER” is the energy transmitted through the outer plate for pass 1, “SOLAR INPUT 1, INNER = TRANSMITTANCE 1, OUTER” is the initial solar irradiance striking the inner plate for pass 1, “ABSORPTANCE 1, INNER” is the energy absorbed by the inner plate for pass 1, “REFLECTANCE 1, IN-

NER" is the energy reflected by the inner plate for pass 1, and "TRANSMITTANCE 1, INNER" is the energy transmitted through the inner plate for pass 1.

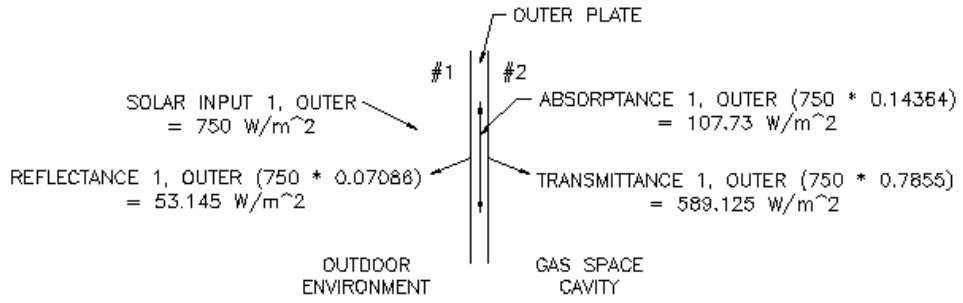

Fig. 13. Summary of ray tracing for outer plate of example IG unit, pass 1

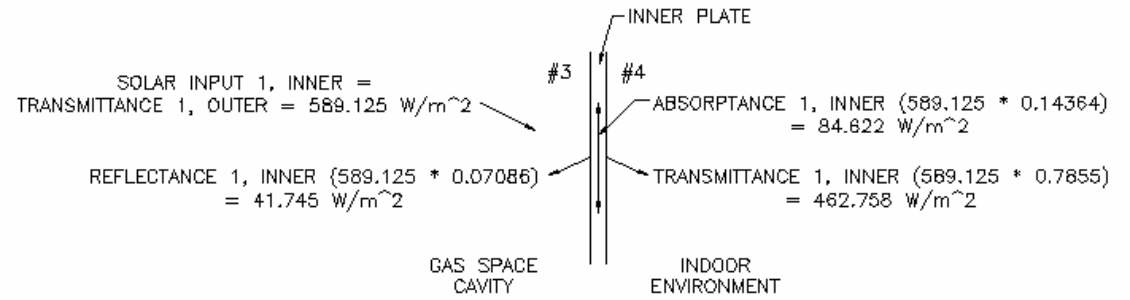

Fig. 14. Summary of ray tracing for inner plate of example IG unit, pass 1

Similar procedures were continued until all of the solar irradiance was absorbed or transmitted. In this case, the ray tracing technique became stable after 3 cycles and it was found that the total absorptance of the outer plate, "Absorptance_Outer," is 113.76 W/m^2, and the total absorptance of the inner plate, "Absorptance_Inner," is 85.05 W/m^2, as summarized in Table 1.

Table 1. Summary of ray tracing for example IG unit

ENERGY	Pass 1	Pass 2	Pass 3	Total
SOLAR INPUT OUTER (W/m^2)	750	41.745	0.21	791.96
ABSORPTANCE OUTER (W/m^2)	107.73	5.996	0.0302	113.76
REFLECTANCE OUTER (W/m^2)	53.145	2.958	0.0149	56.12
TRANSMITTANCE OUTER (W/m^2)	589.125	32.791	0.165	622.08
SOLAR INPUT INNER (W/m^2)	589.125	2.958	0.0149	592.10
ABSORPTANCE INNER (W/m^2)	84.622	0.425	0.00214	85.05
REFLECTANCE INNER (W/m^2)	41.745	0.21	0.00106	41.96
TRANSMITTANCE INNER (W/m^2)	462.758	2.323	0.0117	465.09

Next the initial temperatures of the outer and inner plate for the NPPSA were set to values, previously determined by the ENPP, of 43.5 ^{o}C and 30.9 ^{o}C, respectively. After application of the NPPSA, it was found that the outdoor glass plate reached an equilibrium center of glass temperature of 52.2 ^{o}C and the indoor glass plate reached an equilibrium center of glass temperature of 40.9 ^{o}C.

After the NPPSA produced the transient temperatures, the CEEC procedure was performed. It was found under the given environmental conditions, that the best value of CEEC is 7.30 W/(m^2 K). Fig. 15 shows the variation of temperatures for the more accurate nonlinear propagation procedure and the CEEC procedure. As can be seen in Fig. 15, the CEEC procedure results in little significant error in estimating the variations of the glass plate temperatures with time. These results are typical of a wide range of situations including IG units with and without low-e coatings.

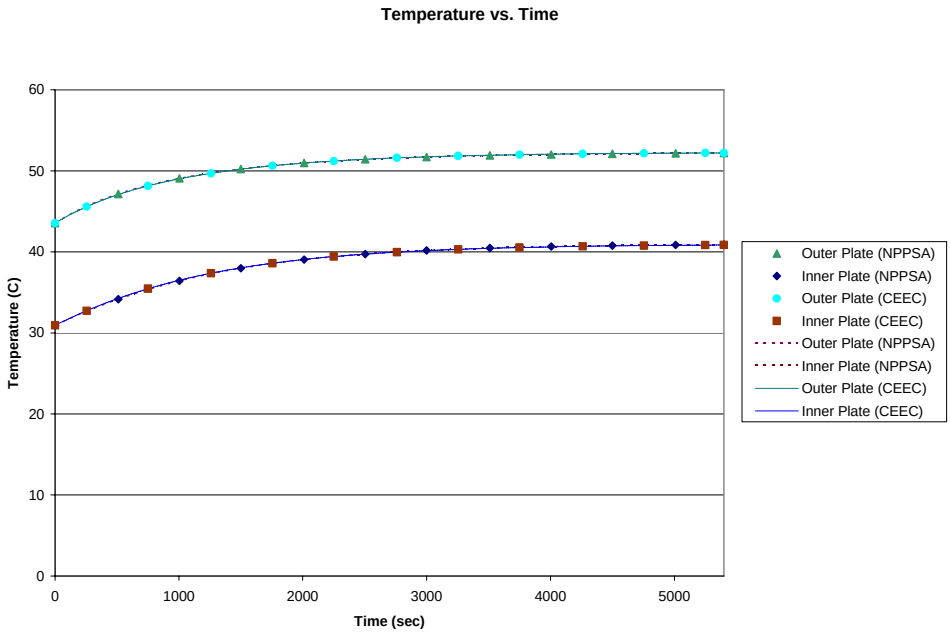

Fig. 15. Variation of outer and inner plate, center of glass temperature, as a function of time for the example IG unit

Results of Numerical Propagation Procedure

The objective of this section was to determine the effect of outdoor temperature and input solar irradiance on CEEC for IG units. It was also desired to determine how the effective emissivity affects the CEEC for IG units with and with out low-e coatings.

The nonlinear least squares regression technique discussed above was used to develop the CEEC for each IG unit examined. For the following results, it was assumed that the environmental conditions consist of a constant indoor temperature of 20 ^{o}C, a constant outdoor total energy exchange coefficient of 13.55 W/(m^2 K), and a constant indoor total energy exchange coefficient of 8.04 W/(m^2 K). The CEEC value was calculated over a range of outdoor temperatures, -10 ^{o}C to 50 ^{o}C, and a range of input solar irradiance, 500 W/m^2 to 1000 W/m^2. An illustration of the environmental conditions are shown in Fig. 16.

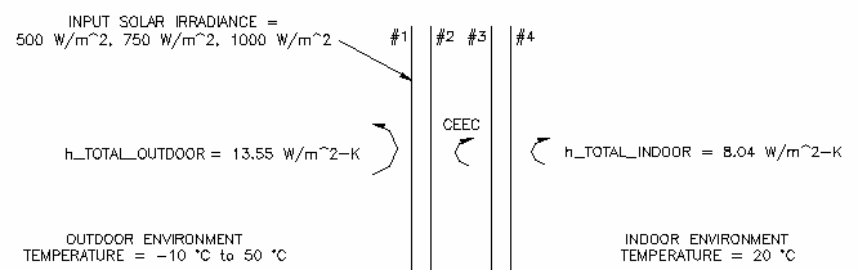

Fig. 16. Environmental conditions for numerical propagation procedure

To develop a better understanding of the variation of CEEC with different types of IG units, 10 IG unit configurations were examined under the previous environmental conditions. The thickness, solar transmittance, solar absorptance, solar reflectance, and emittance properties for 6 single plates are presented in Table 2. Where "Reflectance 1" is the solar reflectance of the #1 or #4 surface, and "Reflectance 2" is the solar reflectance of the surface facing the cavity (#2 or #3). Where "Emissivity 1" is the emissivity of the #1 or #4 surface, and "Emissivity 2" is the emissivity of the surface facing the cavity (#2 or #3).

Table 2. Solar properties for 6 glass plates

Name	Thickness	Transmittance	Absorptance	Reflectance 1	Reflectance 2	Emissivity 1	Emissivity 2
3mm clear	2.97	0.8481269	0.07630174	0.07557136	0.07557136	0.84	0.84
6mm clear	5.66	0.7855316	0.1436073	0.0708611	0.0708611	0.84	0.84
3mm low-e, 1	2.97	0.3419991	0.4183137	0.2396872	0.25824	0.84	0.1017631
6mm low-e, 1	5.66	0.3213857	0.4732485	0.2053658	0.2577013	0.84	0.1017631
3mm low-e, 2	3	0.3789274	0.2544437	0.3666289	0.4669164	0.84	0.0367495
6mm low-e, 2	6	0.3614098	0.3362339	0.3023563	0.4687274	0.84	0.0367495

A combination of the plates presented in Table 2, were used to determine the 10 IG unit cases presented in Table 3.

Table 3. 10 IG unit case studies

Case Number	Outer Glass Plate Name	Inner Glass Plate Name
Case 1	6mm clear	6mm clear
Case 2	3mm clear	3mm clear
Case 3	6mm low-e, 1	6mm clear
Case 4	3mm low-e, 1	3mm clear
Case 5	6mm clear	6mm low-e, 1
Case 6	3mm clear	3mm low-e, 1
Case 7	6mm low-e, 2	6mm clear
Case 8	3mm low-e, 2	3mm clear
Case 9	6mm clear	6mm low-e, 2
Case 10	3mm clear	3mm low-e, 2

Table 4 presents the data used in the calculation of the CEEC for the 10 cases discussed above: where "Thickness_Outer" is the thickness of the outer plate, "Thickness_Inner" is the thickness of the inner plate, "Absorptance_Outer" is the fraction of solar irradiance absorbed by the outer plate determined through ray tracing, "Absorptance_Inner" is the fraction of solar irradiance absorbed by the inner plate determined through ray tracing, "Emissivity 2" is the emissivity of surface #2, and "Emissivity 3" is the emissivity of surface #3.

Table 4. IG unit properties for cases 1 through 10

Case Number	Thickness_Outer (mm)	Thickness_Inner (mm)	Absorptance_Outer	Absorptance_Inner	Emissivity 2	Emissivity 3
Case 1	5.66	5.66	0.1517	0.1134	0.84	0.84
Case 2	2.97	2.97	0.0813	0.0651	0.84	0.84
Case 3	5.66	5.66	0.4830	0.0470	0.101763	0.84
Case 4	2.97	2.97	0.4288	0.0266	0.101763	0.84
Case 5	5.66	5.66	0.1733	0.3368	0.84	0.101763
Case 6	2.97	2.97	0.0934	0.3458	0.84	0.101763
Case 7	6	5.66	0.3407	0.0537	0.03675	0.84
Case 8	3	2.97	0.2591	0.0300	0.03675	0.84
Case 9	5.66	6	0.1983	0.1380	0.84	0.03675
Case 10	2.97	3	0.1077	0.1356	0.84	0.03675

Tables 5 through 14, summarize the calculated CEEC values, for cases 1 through 10, respectively. The CEEC values can be viewed as a function of outdoor temperature and input solar irradiance in Figs. 17 through 26.

Table 5. Summary of case 1 CEEC values

Outdoor Temperature (C)	Equilibrium_CEEC (W/m^2-K)	500_CEEC (W/m^2-K)	750_CEEC (W/m^2-K)	1000_CEEC (W/m^2-K)
-10.0	5.51118	5.69878	5.79745	5.89881
-5.0	5.60699	5.79889	5.90037	6.00477
0.0	5.70797	5.90479	6.00928	6.11702
5.0	5.81377	6.01620	6.12420	6.23592
10.0	5.92402	6.13316	6.24570	6.36270
15.0	6.03836	6.25815	6.37868	6.50466
20.0	6.15692	6.40581	6.53406	6.66469
25.0	6.27769	6.47724	6.56182	6.63406
30.0	6.40248	6.61717	6.71814	6.81467
35.0	6.53089	6.75442	6.86178	6.96705
40.0	6.66296	6.89381	7.00514	7.11544
45.0	6.79867	7.03616	7.15064	7.26468
50.0	6.93797	7.18270	7.30002	7.41730
Average CEEC (W/m^2-K)	6.42570			
Max % Error	16.6			

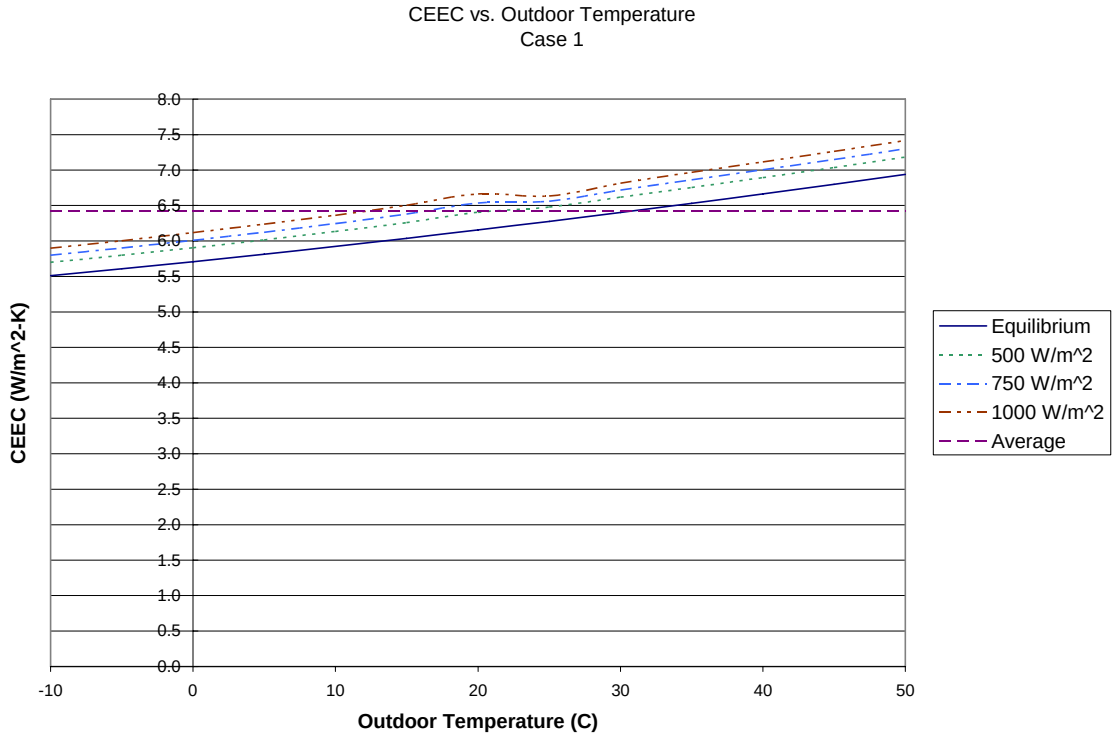

Fig. 17. CEEC versus outdoor temperature, case 1, 6 mm clear outer plate and 6 mm clear inner plate

Table 6. Summary of case 2 CEEC values

Outdoor Temperature (C)	Equilibrium_CEEC (W/m^2-K)	500_CEEC (W/m^2-K)	750_CEEC (W/m^2-K)	1000_CEEC (W/m^2-K)
-10.0	5.51118	5.62769	5.68818	5.74955
-5.0	5.60699	5.72564	5.78757	5.85045
0.0	5.70797	5.82921	5.89262	5.95704
5.0	5.81377	5.93798	6.00298	6.06910
10.0	5.92402	6.05169	6.11850	6.18661
15.0	6.03836	6.17065	6.24009	6.31103
20.0	6.15851	6.30140	6.37514	6.44970
25.0	6.27769	6.40885	6.46922	6.52412
30.0	6.40248	6.54042	6.60699	6.67237
35.0	6.53089	6.67379	6.74287	6.81159
40.0	6.66296	6.81055	6.88138	6.95219
45.0	6.79867	6.95104	7.02341	7.09594
50.0	6.93797	7.09517	7.16896	7.24302
Average CEEC (W/m^2-K)	6.33396			
Max % Error	14.9			

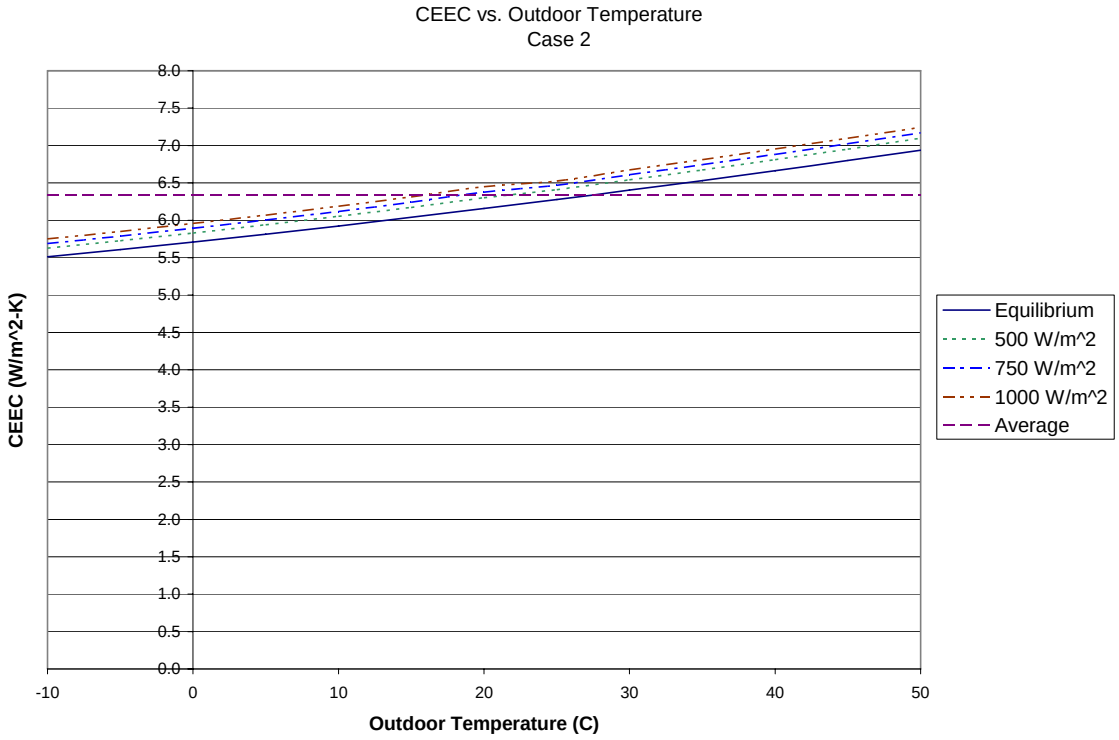

Fig. 18. CEEC versus outdoor temperature, case 2, 3 mm clear outer plate and 3 mm clear inner plate

Table 7. Summary of case 3 CEEC values

Outdoor Temperature (C)	Equilibrium_CEEC (W/m^2-K)	500_CEEC (W/m^2-K)	750_CEEC (W/m^2-K)	1000_CEEC (W/m^2-K)
-10.0	2.58575	2.56292	2.57062	2.55742
-5.0	2.55039	2.56732	2.56444	2.61536
0.0	2.55044	2.57303	2.58900	2.64979
5.0	2.55516	2.56520	2.63385	2.67216
10.0	2.56399	2.61885	2.65433	2.69646
15.0	2.57633	2.63740	2.67698	2.72399
20.0	2.59139	2.65873	2.70317	2.75489
25.0	2.60832	2.68373	2.73284	2.83905
30.0	2.62768	2.71226	2.78344	2.93401
35.0	2.64983	2.74416	2.88148	3.02390
40.0	2.67488	2.82811	2.97509	3.10900
45.0	2.70287	2.92571	3.06358	3.18984
50.0	2.73375	3.01842	3.14765	3.26713
Average CEEC (W/m^2-K)	2.73223			
Max % Error	16.4			

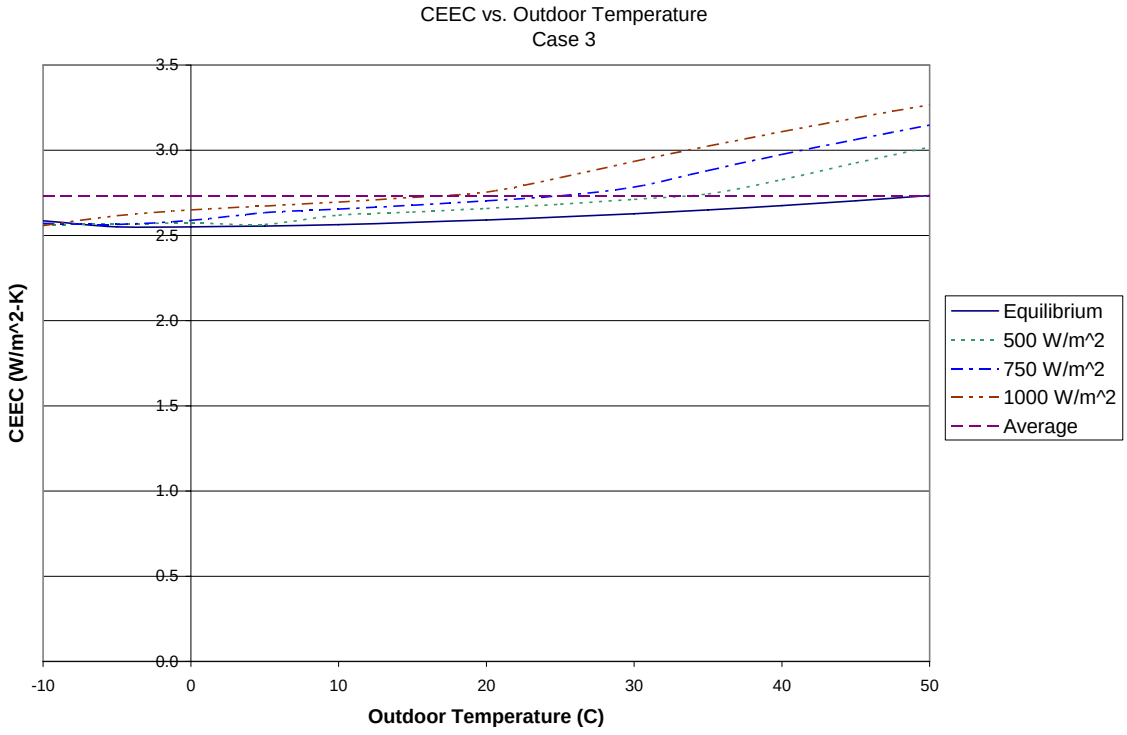

Fig. 19. CEEC versus outdoor temperature, case 3, 6 mm clear with low-e, 1 outer plate and 6 mm clear inner plate

Table 8. Summary of case 4 CEEC values

Outdoor Temperature (C)	Equilibrium_CEEC (W/m^2-K)	500_CEEC (W/m^2-K)	750_CEEC (W/m^2-K)	1000_CEEC (W/m^2-K)
-10.0	2.60247	2.56168	2.57205	2.56326
-5.0	2.55402	2.56715	2.57376	2.60145
0.0	2.55267	2.57548	2.57445	2.63602
5.0	2.55637	2.56945	2.62399	2.65822
10.0	2.56453	2.61258	2.64460	2.68255
15.0	2.57648	2.63161	2.66753	2.71010
20.0	2.59139	2.65327	2.69381	2.74094
25.0	2.60832	2.67836	2.72346	2.80308
30.0	2.62785	2.70685	2.75843	2.90319
35.0	2.65040	2.73862	2.85859	2.99654
40.0	2.67609	2.81303	2.95522	3.08405
45.0	2.70493	2.91321	3.04559	3.16661
50.0	2.73687	3.00674	3.13055	3.24489
Average CEEC (W/m^2-K)	2.72391			
Max % Error	16.1			

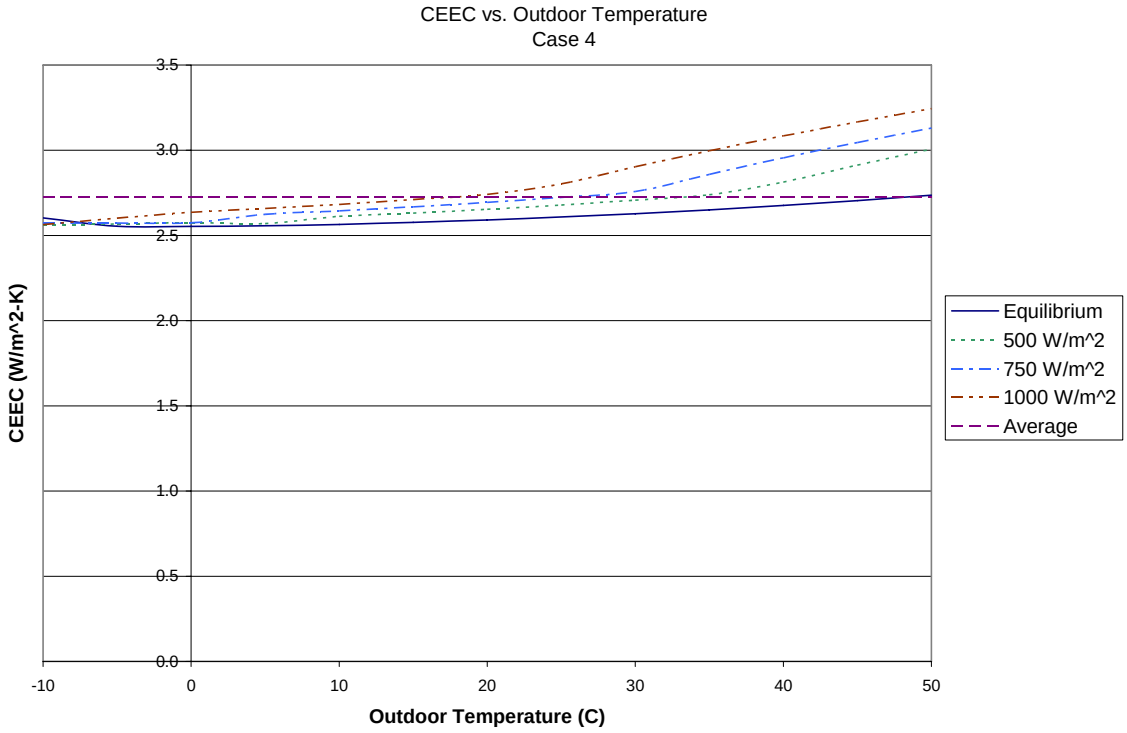

Fig. 20. CEEC versus outdoor temperature, case 4, 3 mm clear with low-e, 1 outer plate and 3 mm clear inner plate

Table 9. Summary of case 5 CEEC values

Outdoor Temperature (C)	Equilibrium_CEEC (W/m^2-K)	500_CEEC (W/m^2-K)	750_CEEC (W/m^2-K)	1000_CEEC (W/m^2-K)
-10.0	2.58574	2.86425	2.97645	3.08188
-5.0	2.55039	2.78399	2.90591	3.01942
0.0	2.55044	2.70314	2.83285	2.95459
5.0	2.55516	2.64841	2.76077	2.88856
10.0	2.56400	2.64979	2.70413	2.82337
15.0	2.57633	2.65623	2.70555	2.76850
20.0	2.59146	2.66762	2.71402	2.76591
25.0	2.60832	2.68343	2.72713	2.77612
30.0	2.62769	2.68191	2.74220	2.79001
35.0	2.64983	2.68160	2.73178	2.80229
40.0	2.67488	2.71504	2.71342	2.78451
45.0	2.70287	2.74332	2.75313	2.75248
50.0	2.73375	2.77195	2.78791	2.78915
Average CEEC (W/m^2-K)	2.73603			
Max % Error	11.2			

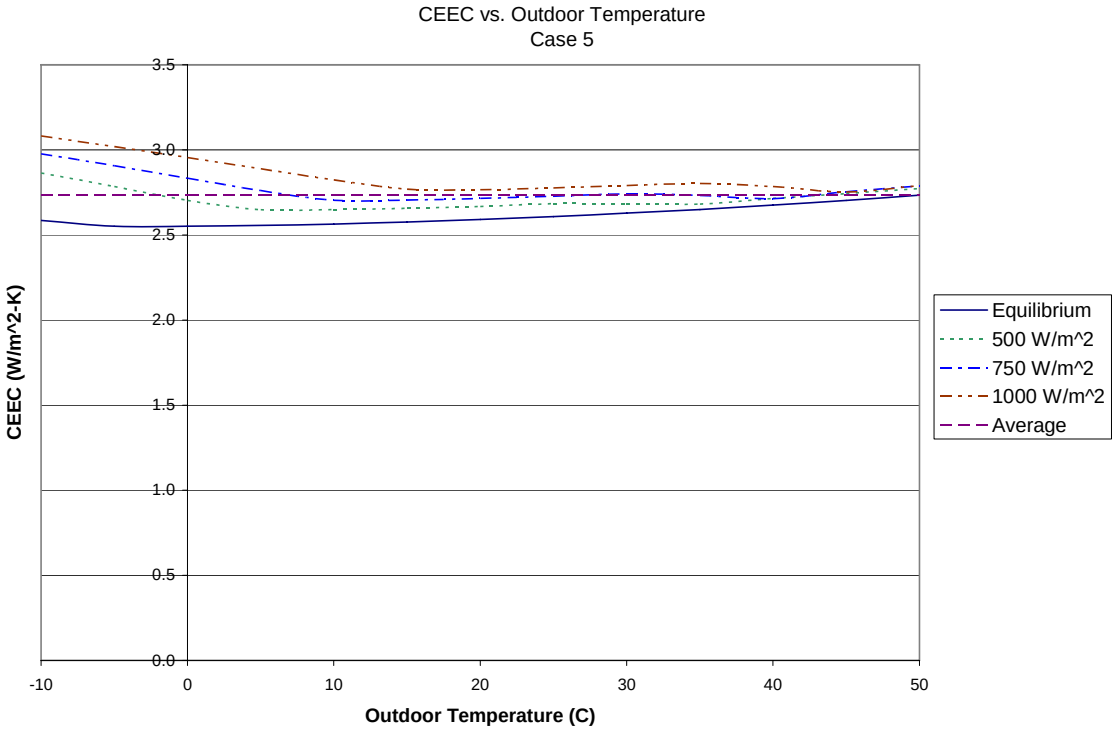

Fig. 21. CEEC versus outdoor temperature, case 5, 6 mm clear outer plate and 6 mm clear with low-e, 1 inner plate

Table 10. Summary of case 6 CEEC values

Outdoor Temperature (C)	Equilibrium_CEEC (W/m^2-K)	500_CEEC (W/m^2-K)	750_CEEC (W/m^2-K)	1000_CEEC (W/m^2-K)
-10.0	2.58574	2.94701	3.08602	3.21263
-5.0	2.55040	2.87355	3.02307	3.15782
0.0	2.55045	2.79534	2.95657	3.10043
5.0	2.55516	2.71373	2.88636	3.04024
10.0	2.56399	2.66457	2.81251	2.97686
15.0	2.57633	2.66618	2.73864	2.91002
20.0	2.59145	2.67259	2.72763	2.84053
25.0	2.60832	2.68329	2.73343	2.79289
30.0	2.62768	2.69683	2.74330	2.79814
35.0	2.64983	2.69280	2.75569	2.80721
40.0	2.67488	2.70284	2.76124	2.81860
45.0	2.70287	2.73738	2.73389	2.82669
50.0	2.73375	2.76535	2.76811	2.81067
Average CEEC (W/m^2-K)	2.77695			
Max % Error	13.6			

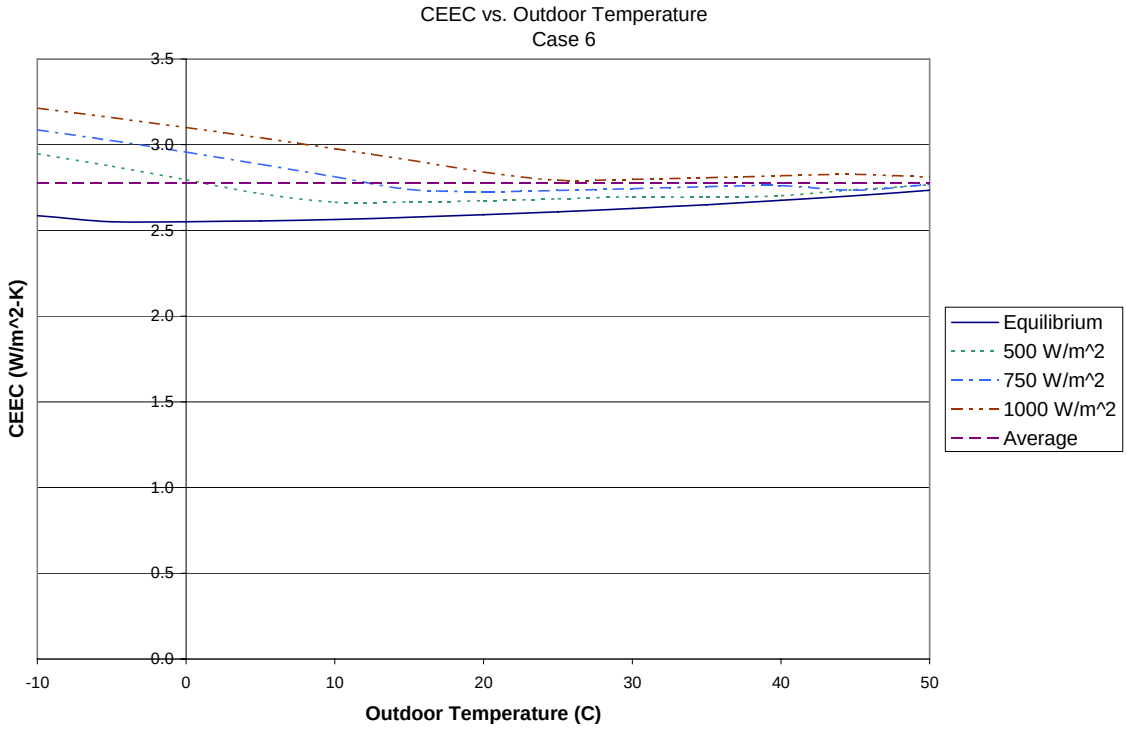

Fig. 22. CEEC versus outdoor temperature, case 6, 3 mm clear outer plate and 3 mm clear with low-e, 1 inner plate

Table 11. Summary of case 7 CEEC values

Outdoor Temperature (C)	Equilibrium_CEEC (W/m^2-K)	500_CEEC (W/m^2-K)	750_CEEC (W/m^2-K)	1000_CEEC (W/m^2-K)
-10.0	2.30075	2.24220	2.23688	2.23591
-5.0	2.24003	2.23183	2.23066	2.23179
0.0	2.22968	2.22784	2.22926	2.22748
5.0	2.22409	2.22758	2.22589	2.24277
10.0	2.22269	2.22597	2.24269	2.25399
15.0	2.22485	2.24069	2.25146	2.26501
20.0	2.23368	2.24912	2.26281	2.27940
25.0	2.23643	2.26099	2.27767	2.29727
30.0	2.24556	2.27637	2.29605	2.31861
35.0	2.25752	2.29530	2.31792	2.39763
40.0	2.27249	2.31773	2.40289	2.48699
45.0	2.29049	2.40934	2.49318	2.57072
50.0	2.31328	2.50090	2.57754	2.64886
Average CEEC (W/m^2-K)	2.29805			
Max % Error	2.6			

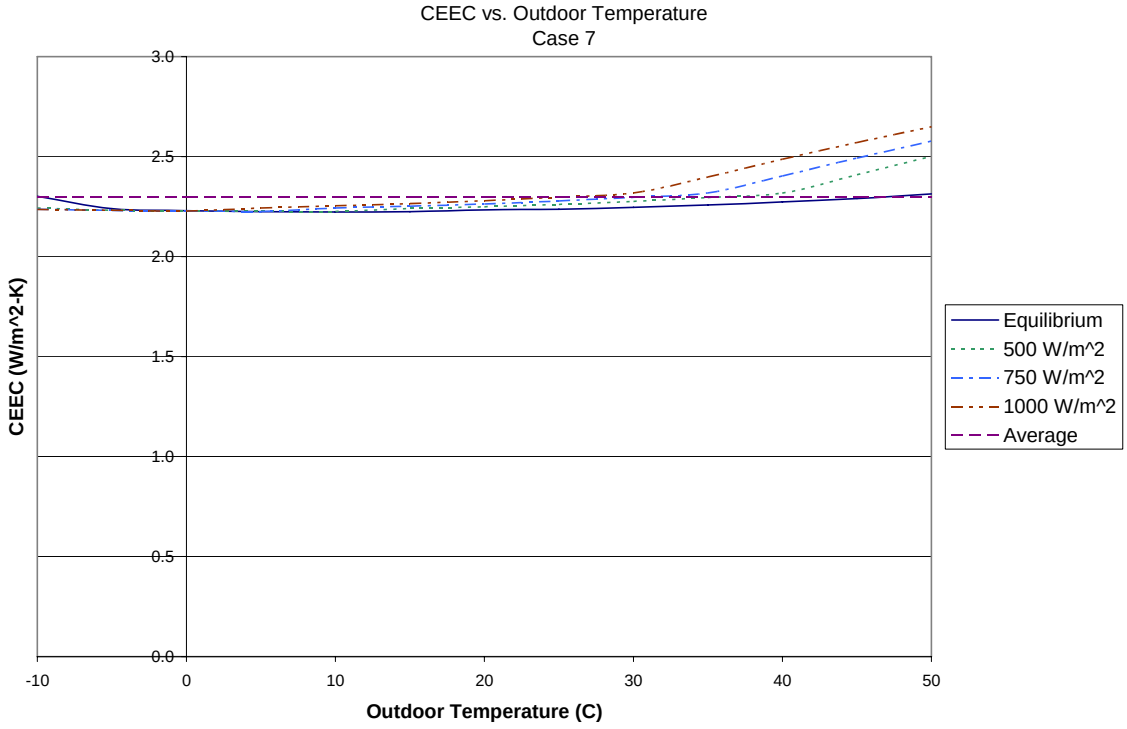

Fig. 23. CEEC versus outdoor temperature, case 7, 6 mm clear with low-e, 2 outer plate and 6 mm clear inner plate

Table 12. Summary of case 8 CEEC values

Outdoor Temperature (C)	Equilibrium_CEEC (W/m^2-K)	500_CEEC (W/m^2-K)	750_CEEC (W/m^2-K)	1000_CEEC (W/m^2-K)
-10.0	2.32176	2.24305	2.23652	2.23339
-5.0	2.24410	2.23215	2.22966	2.22976
0.0	2.23212	2.22721	2.22793	2.22990
5.0	2.22536	2.22662	2.22898	2.22537
10.0	2.22320	2.22871	2.23464	2.24425
15.0	2.22496	2.23657	2.24437	2.25392
20.0	2.23077	2.24457	2.25467	2.26677
25.0	2.23650	2.25574	2.26839	2.28307
30.0	2.24593	2.27035	2.28558	2.30284
35.0	2.25850	2.28847	2.30627	2.33770
40.0	2.27436	2.31008	2.35964	2.43399
45.0	2.29355	2.38185	2.45487	2.52278
50.0	2.32160	2.47610	2.54246	2.60457
Average CEEC (W/m^2-K)	2.28839			
Max % Error	2.6			

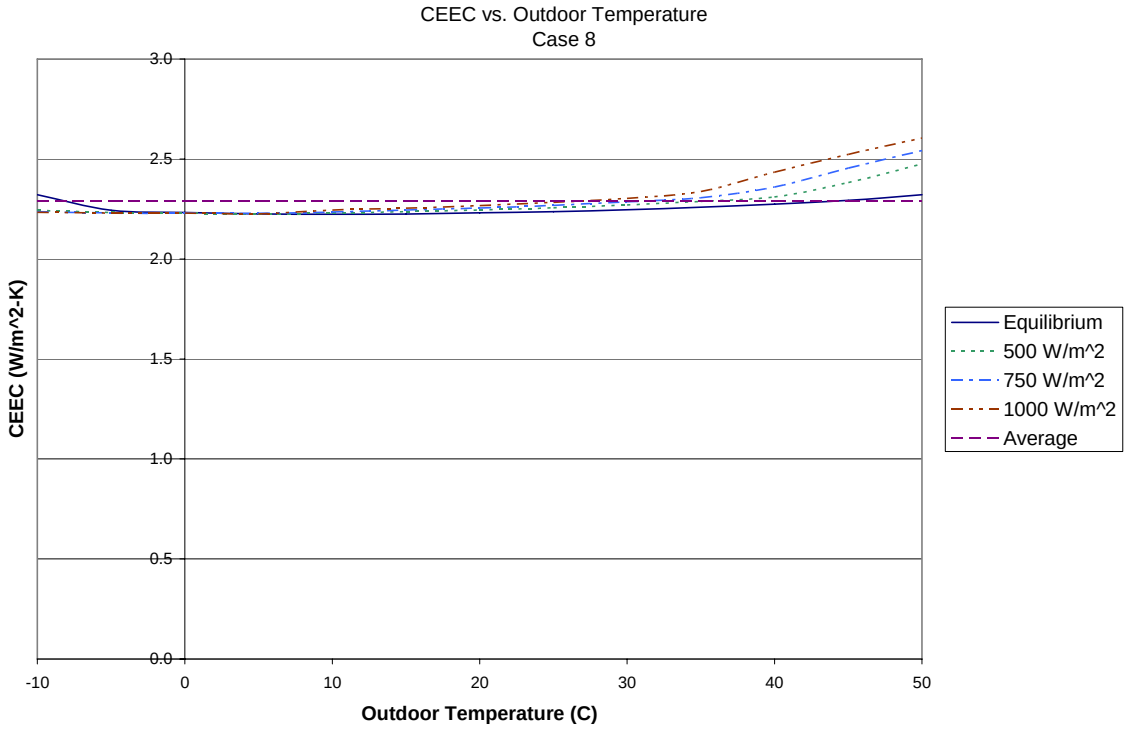

Fig. 24. CEEC versus outdoor temperature, case 8, 3 mm clear with low-e, 2 outer plate and 3 mm clear inner plate

Table 13. Summary of case 9 CEEC values

Outdoor Temperature (C)	Equilibrium_CEEC (W/m^2-K)	500_CEEC (W/m^2-K)	750_CEEC (W/m^2-K)	1000_CEEC (W/m^2-K)
-10.0	2.29926	2.33354	2.33323	2.33343
-5.0	2.23964	2.25721	2.26288	2.26888
0.0	2.22940	2.24529	2.25157	2.25819
5.0	2.22390	2.23870	2.24548	2.25262
10.0	2.22258	2.23678	2.24404	2.25170
15.0	2.22480	2.23909	2.24700	2.25546
20.0	2.23014	2.24254	2.24918	2.25597
25.0	2.23647	2.24934	2.25539	2.26121
30.0	2.24562	2.25949	2.26617	2.27281
35.0	2.25760	2.27251	2.27937	2.28629
40.0	2.27255	2.28879	2.29566	2.30265
45.0	2.29053	2.30842	2.31518	2.32212
50.0	2.31288	2.33778	2.34586	2.35428
Average CEEC (W/m^2-K)	2.27041			
Max % Error	3.6			

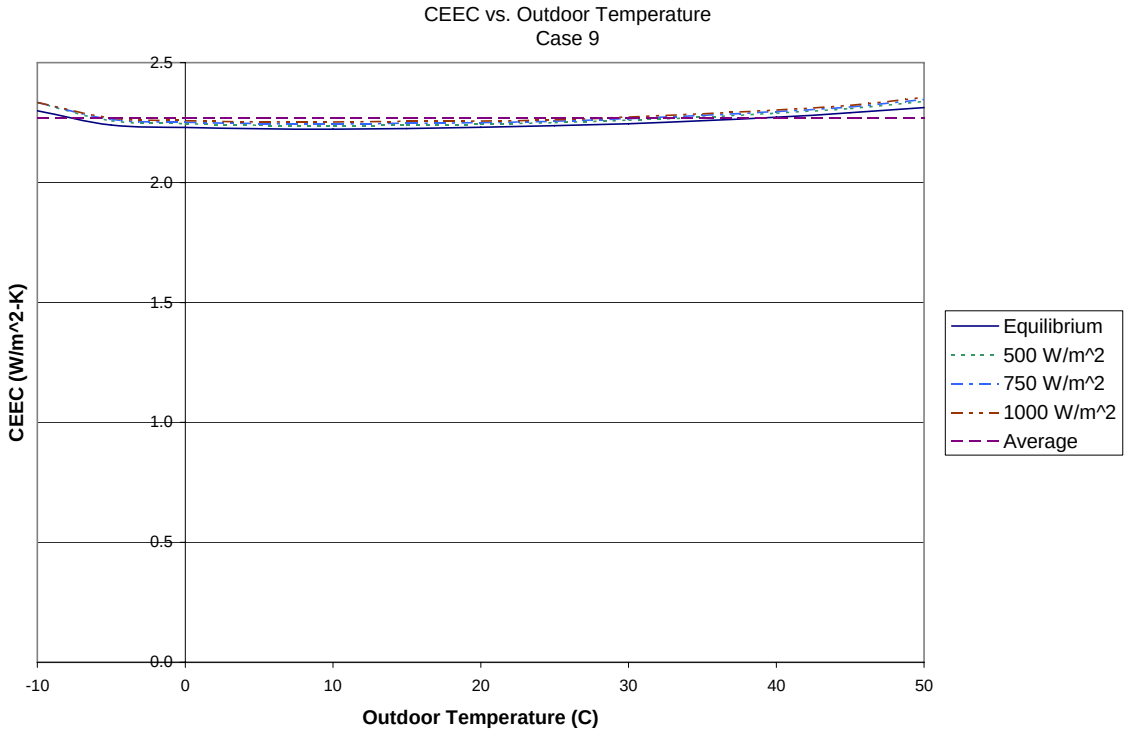

Fig. 25. CEEC versus outdoor temperature, case 9, 6 mm clear outer plate and 6 mm clear with low-e, 2 inner plate

Table 14. Summary of case 10 CEEC values

Outdoor Temperature (C)	Equilibrium_CEEC (W/m^2-K)	500_CEEC (W/m^2-K)	750_CEEC (W/m^2-K)	1000_CEEC (W/m^2-K)
-10.0	2.32163	2.41382	2.45077	2.48645
-5.0	2.24407	2.30802	2.34958	2.38965
0.0	2.23210	2.25621	2.26850	2.29295
5.0	2.22534	2.24587	2.25681	2.26843
10.0	2.22319	2.24059	2.25024	2.26059
15.0	2.22496	2.23982	2.24830	2.25745
20.0	2.23081	2.24300	2.25047	2.25852
25.0	2.23650	2.24355	2.25128	2.26200
30.0	2.24594	2.25454	2.25822	2.25899
35.0	2.25850	2.26539	2.26927	2.27305
40.0	2.27436	2.27918	2.28215	2.28560
45.0	2.29355	2.29621	2.29796	2.30046
50.0	2.32154	2.31665	2.31701	2.31828
Average CEEC (W/m^2-K)	2.28074			
Max % Error	8.3			

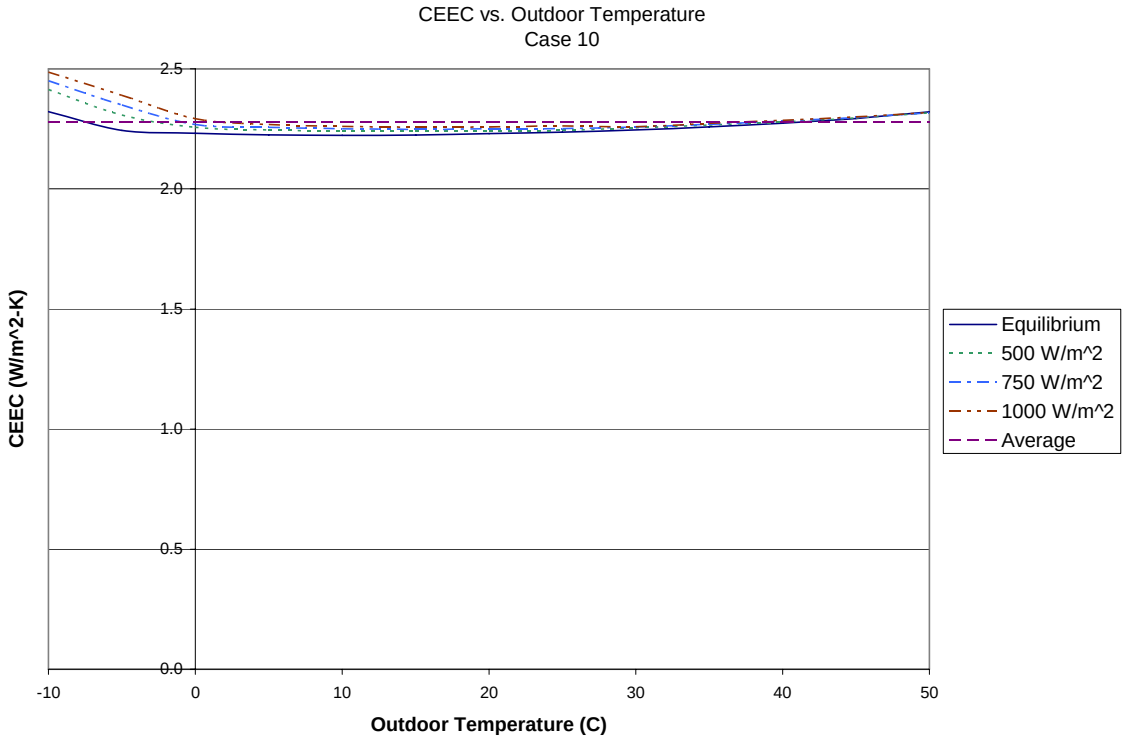

Fig. 26. CEEC versus outdoor temperature, case 10, 3 mm clear outer plate and 3 mm clear with low-e, 2 inner plate

The CEEC value for case 1 (6 mm clear outer plate and 6 mm clear inner plate) and case 2 (3 mm clear outer plate and 3 mm clear inner plate) increases linearly with respect to an increase in outdoor temperature from approximately 5.5 W/(m^2 K) at -10 ^oC to 7.4 W/(m^2 K) at 50 ^oC. Also, the CEEC value slightly increases with an increase in solar irradiance.

The CEEC value for case 3 (6 mm low-e, 1 outer plate and 6 mm clear inner plate) and case 4 (3 mm low-e, 1 outer plate and 3 mm clear inner plate) remains relatively constant with respect to outdoor temperature ranging from approximately 2.6 W/(m^2 K) at -10 ^oC to 3.3 W/(m^2 K) at 50 ^oC. The relatively constant CEEC value is primarily because the radiation exchange is greatly reduced by the use of a low-e coating and energy exchange is primarily due to conduction and natural convection.

The results suggest that if the low-e coating is placed on the #2 surface and the IG unit is placed in hot environmental conditions (outdoor temperature greater than 20 ^oC), the CEEC value varies more than if placed in cold environmental conditions (outdoor temperature less than 20 ^oC). This is the case because if the low-e coating is placed on the #2 surface the outer plate will absorb more solar irradiance. The increase in absorbed solar irradiance combined with hot outdoor environmental conditions results in larger outer plate temperatures, as will be shown in Chapter V. The larger outer plate temperature ultimately results in a larger temperature difference between the outer glass plate and inner glass plate, which increases the energy exchange through the gas space cavity.

Results similar to cases 3 and 4 are discovered for cases 5 and 6, where the low-e coating is placed on the #3 surface, with the exception that the CEEC value varies more when the IG unit is placed in cold environmental conditions. Cases 7 through 10 are the same as cases 3 through 6, with the exception that the emissivity of the low-e coating used in the analysis is reduced, which results in a reduced CEEC value.

CHAPTER V

FINITE ELEMENT ANALYSIS

The purpose of this chapter is to develop understandings of thermal stresses in insulating glass (IG) units and how these IG thermal stresses compare to those that develop in a monolithic glass plate under similar environmental conditions. In this effort it will be assumed that the energy exchange through the gas space cavity is well modeled with the cavity energy exchange coefficient (CEEC) developed in chapter IV. Using this assumption, a transient finite element analysis is used to determine the variation between the center of glass temperature (T_{CGA}) and perimeter of glass temperature (T_{PG}) as a function of time for a range of cases, given a specified set of environmental conditions. Finally, thermal stresses are estimated based on the T_{CGA} to T_{PG} temperature difference.

The finite element analysis is conducted in three major steps. First, the model geometry is defined, next an equilibrium analysis is performed, and finally the transient analysis is performed. The transient analysis results in the T_{CGA}'s and T_{PG}'s as a function of time. The T_{CGA}'s and T_{PG}'s are then used to determine the maximum thermal stress for a set of case studies involving both IG units and monolithic glass plates. This procedure is discussed in detail in the next section. Finally, results of the FEA analysis are presented.

General Procedure for Determining Maximum Thermal Stress in Window Glass

The finite element package ALGOR 13.30 was the computational tool used to determine the T_{CGA}'s and T_{PG}'s as a function of time (ALGOR 2003). The geometry and mesh was constructed using ALGOR's graphical user interface, Super Draw III. The first step in the finite element analysis (FEA) was to construct the model that represents the window being studied. The heat transfer through the center of glass area is one-dimensional

while the heat transfer through the edge of glass area is two-dimensional, thus a two-dimensional model was used (Wright and Sullivan 1995; Manz 2003; ASHRAE 2005; Gordon 2001; Isamil and Henriquez 2005).

One of the critical factors in the development of thermal stresses in glass plates is the frame type and edge bite. ASTM 2431-06 (ASTM 2006) presents three frame types for the design of monolithic glass plates. For this thesis, the frame type was chosen to be perfectly insulated, which represents the best frame condition for monolithic glass. Based on this, it was assumed that energy does not flow between the IG unit and the frame. Thus, energy flows to the perimeter of glass solely due to conduction from the center of glass area. An edge bite was used to model the part of the frame that shades the edge of glass from solar irradiance. For purposes of this thesis the edge bite distance was taken to be 19.05 mm.

The geometry of a finite element model is made up of nodes and elements which ultimately define the finite element mesh. For this thesis, rectangular elements were used in the construction of the two dimensional finite element model. Sufficient length was needed to accommodate the transition in temperature from the T_{CGA} to the T_{PG}. For this thesis, the model length was chosen to be 323.85 mm. In addition, it was determined that nodes spaced at 6.35 mm in the longitudinal direction, and nodes at $t_{GL}/2$, in the transverse direction were sufficient to accommodate all cases considered, where t_{GL} is the thickness of the glass plate.

The next step in developing the finite element model was to define the material properties of all of the elements involved. The material properties used in thermal analyses include the specific heat, thermal conductivity, and density. Table 15, presents a list of the material properties for glass, steel, and silicone.

Table 15. Material properties for glass, steel, and silicone

	Specific Heat (J/(kg K))	Thermal Conductivity (W/(m K))	Density (kg/m^3)
Glass	838.3	1.0208	2511.9
Steel	499.87	46.76	7855
Silicone	0.00146	0.31	48.74

To develop understandings of the thermal stress behavior of windows in a variety of cases, a reasonable set of solar irradiance and temperature values were established for the parameter study. In this study, three different solar irradiance inputs were examined as follows: 500 W/m^2, 750 W/m^2, and 1000 W/m^2. Three different outdoor temperatures were considered as follows: -10 ^oC, 20 ^oC, and 50 ^oC . This results in a total of nine different combinations for each case. For all cases considered, the indoor temperature was held constant at 20 ^oC. The outdoor total energy exchange coefficient was held constant at 13.55 $W/(m^2 K)$ as given by Beason and Lingnell (2002). The indoor total energy exchange coefficient was held constant at 8.04 W/m^2-K as given by Beason and Lingnell (2002). In addition, it was assumed that the solar irradiance is absorbed evenly at all points through the thickness of the glass (Wright 1998; Powles et al. 2002).

In addition to the environmental conditions, the gas space energy exchange for windows involving IG units was modeled using the CEEC. The CEEC for a particular situation was determined using the previously defined material properties and environmental conditions, and the numerical propagation procedure developed in Chapter IV. The CEEC determined from the numerical propagation procedure was then converted to an effective conductance by multiplying the CEEC by the gas space thickness. The effective conductance was then used to model the total energy exchange through the gas space cavity (Gordon 2001; Gustavsen et al. 2005). For cases involving IG units the gas space thickness was taken to be 12.93 mm. Figs. 27 and 28, illustrate the use of these environmental conditions for a monolithic glass plate and IG unit, respectively.

The CEEC will experience local effects at the frame because of the energy exchange between the spacer and the gas space cavity (Wright 1996). However, for this thesis the local effects of the spacer on the CEEC value were neglected in accordance with Muneer (et al. 1997). Muneer (et al. 1997) found that for windows with air infill the change in convection due to the spacer is negligible; but for other infill gases the change in convection might be significant.

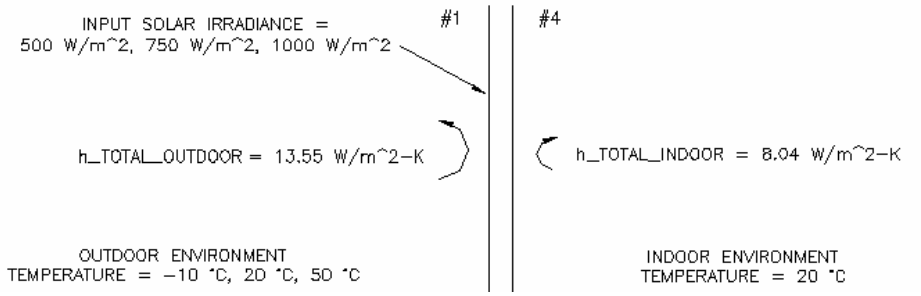

Fig. 27. Environmental conditions for monolithic glass plate

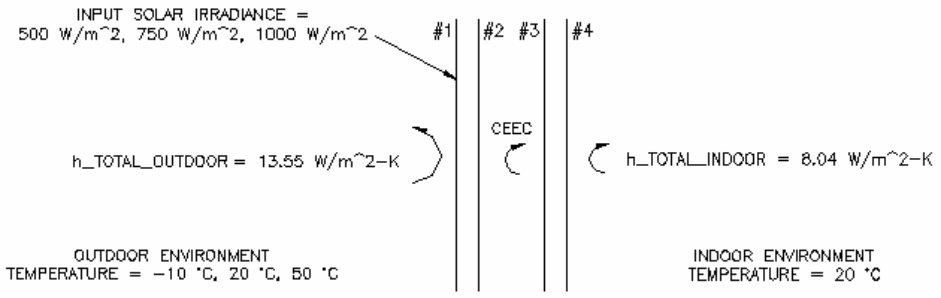

Fig. 28. Environmental conditions for IG unit

To model the development of thermal stresses in window glass, it is first necessary to determine the equilibrium temperatures that develop in the glass based on the indoor and outdoor environmental conditions, without solar irradiance. The analysis to determine the equilibrium temperatures will be referred to as the equilibrium analysis (EA). Ex-

amples of the T_{CGA} and T_{PG} for an equilibrium analysis are presented in Figs. 29 and 30 for a monolithic glass plate and an IG unit, respectively. The plates in both cases are clear glass plates with a thickness of 6 mm. The environmental conditions used to determine the T_{CGA} and T_{PG} for the EA are as previously defined, with an outdoor temperature of 10 ^{o}C and indoor temperature of 20 ^{o}C.

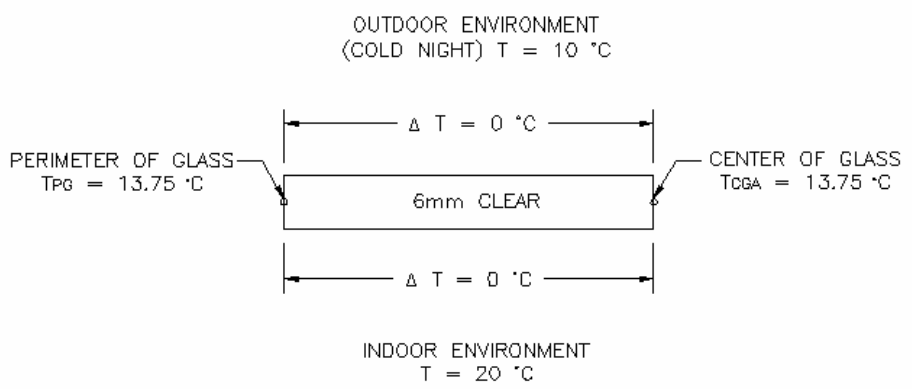

Fig. 29. T_{CGA} and T_{PG} for monolithic glass plate

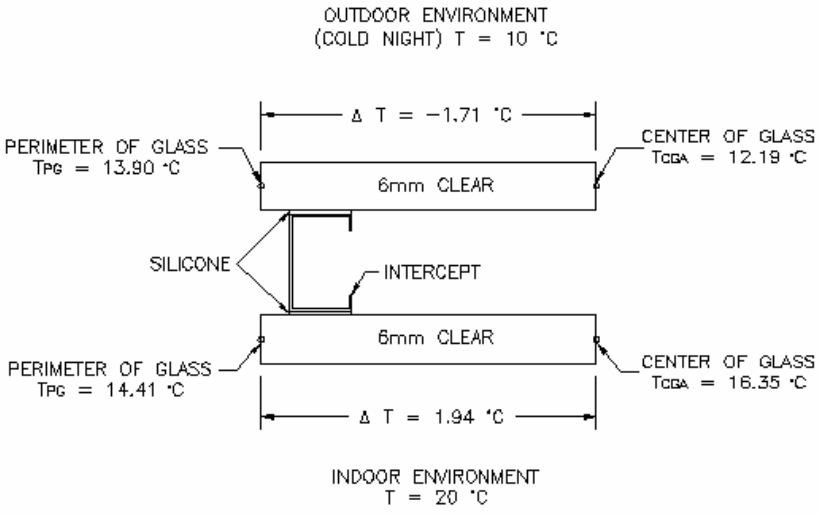

Fig. 30. T_{CGA} and T_{PG} for IG unit

The temperatures from the EA are then used as the initial temperatures in the transient analysis to determine the variation of the T_{CGA}'s and T_{PG}'s with time. This will be referred to as the transient analysis (TA). From these data, the difference in T_{CGA} and T_{PG} was determined for each time step in the FEA analysis. As previously stated, a time step of 15 seconds was determined to be sufficient.

The maximum thermal edge stress that develops in the glass is proportional to the maximum temperature difference between the T_{CGA} and T_{PG} (Turner 1977; Wright and Barry 1999; Zhong-wei et al. 1999; Pilkington 2005). The maximum thermal stress can be approximated by multiplying the maximum difference in T_{CGA} and T_{PG} by the product of the thermal coefficient of expansion of the glass, α_T, and Young's modulus, E. For the case of international system of units, α_T * E is approximately equal to 0.632394 MPa/K. The resulting relationship to estimate the thermal stress for a given instant is then given by Eq. (35).

$$\sigma = \alpha_T \, E \, (T_{CGA} - T_{PG}) = 0.632394 \, (T_{CGA} - T_{PG}) \, (\text{Mpa}) \qquad (35)$$

Where σ is the thermal perimeter stress, the coefficient of thermal expansion for glass α_T is taken to be 8.82 x 10^{-6} m/m/K, and Young's modulus of glass E is taken to be 71.7 GPa (Beason and Lingnell 2002). If the T_{CGA} exceeds the T_{PG}, the stress along the perimeter of glass is positive and is associated with a tensile stress, while negative implies compressive stresses.

This general FEA procedure for determining maximum thermal stress was applied to eight case studies involving both monolithic glass plates and IG units, with different glass thicknesses and gas space cavity emissivities as described below. These cases were selected to develop understandings of how thermal stresses develop in IG units and how they compare to thermal stresses that develop in monolithic glass plates given the same environmental conditions.

All cases studied were fabricated with various combinations of four different types of glass plates. The thickness, solar transmittance, solar absorptance, solar reflectance, and emittance properties for these four glass plates are presented in Table 16: where "Reflectance 1" is the solar reflectance of the #1 or #4 surface and "Reflectance 2" is the solar reflectance of the surface facing the cavity (#2 or #3),"Emissivity 1" is the emissivity of the #1 or #4 surface, and "Emissivity 2" is the emissivity of the surface facing the cavity (#2 or #3).

Table 16. Solar properties for 4 glass plates

Name	Thickness (mm)	Transmittance	Absorptance	Refelctance 1	Reflectance 2	Emissivity 1	Emissivity 2
3mm clear	3	0.8481269	0.07630174	0.07557136	0.07557136	0.84	0.84
6mm clear	6	0.7855316	0.1436073	0.0708611	0.0708611	0.84	0.84
3mm low-e, 2	3	0.3789274	0.2544437	0.3666289	0.4669164	0.84	0.0367495
6mm low-e, 2	6	0.3614098	0.3362339	0.3023563	0.4687274	0.84	0.0367495

Eight different window configurations were selected for study using the glass plate properties presented in Table 16. The first two cases studied represent monolithic glass and the last six cases represent different IG unit configurations. All of the different cases are summarized in Table 17.

Table 17. 8 FEA case studies

Case Number	Outer Glass Plate Name	Inner Glass Plate Name	Comment
FEA Case 1	6mm clear	N/A	Monolithic Glass Plate
FEA Case 2	3mm clear	N/A	Monolithic Glass Plate
FEA Case 3	6mm clear	6mm clear	IG Unit
FEA Case 4	3mm clear	3mm clear	IG Unit
FEA Case 5	6mm low-e, 2	6mm clear	IG Unit
FEA Case 6	3mm low-3, 2	3mm clear	IG Unit
FEA Case 7	6mm clear	6mm low-e, 2	IG Unit
FEA Case 8	3mm clear	3mm low-e, 2	IG Unit

Table 18, presents the data used in the finite element analysis for the cases discussed above: where "Absorptance_Outer" is the fraction of solar irradiance absorbed by the outer plate, and "Absorptance_Inner" is the fraction of solar irradiance absorbed by the inner plate.

Table 18. FEA data for cases 1 through 8

Case Number	Absorptance_Outer	Absorptance_Inner	CEEC -10 °C (W/m^2-K)	CEEC 20 °C (W/m^2-K)	CEEC 50 °C (W/m^2-K)
FEA Case 1	0.1436	N/A	N/A	N/A	N/A
FEA Case 2	0.0763	N/A	N/A	N/A	N/A
FEA Case 3	0.1517	0.1134	5.67	6.39	7.16
FEA Case 4	0.0813	0.0651	5.57	6.23	7.06
FEA Case 5	0.3407	0.0537	2.09	2.12	2.56
FEA Case 6	0.2591	0.0300	2.11	2.11	2.53
FEA Case 7	0.1983	0.1380	2.31	2.11	2.29
FEA Case 8	0.1077	0.1356	2.44	2.11	2.20

Monolithic Glass Plate Case Study Results

Fig. 31 illustrates the geometry and mesh for a monolithic glass plate that was used in the finite element analysis. The monolithic geometry consists of a single glass plate 323.85 mm long, with a thickness, t_{GL}, and a 19.05 mm edge bite. A convergence study was conducted to determine the proper nodal spacing for the current problem. It was found that a mesh with nodes at 6.35 mm in the longitudinal direction and $t_{GL}/2$ in the transverse direction was sufficient to estimate the transient temperatures for all cases.

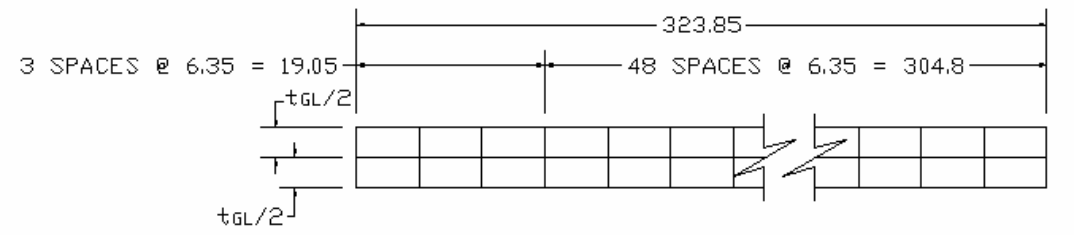

Fig. 31. Finite element geometry and mesh, monolithic glass plate

Once the geometry, mesh, and properties were defined, the next step was to perform the EA and TA, the results of which are presented in Figs. 32 and 33 for FEA case 1 and FEA case 2, respectively.

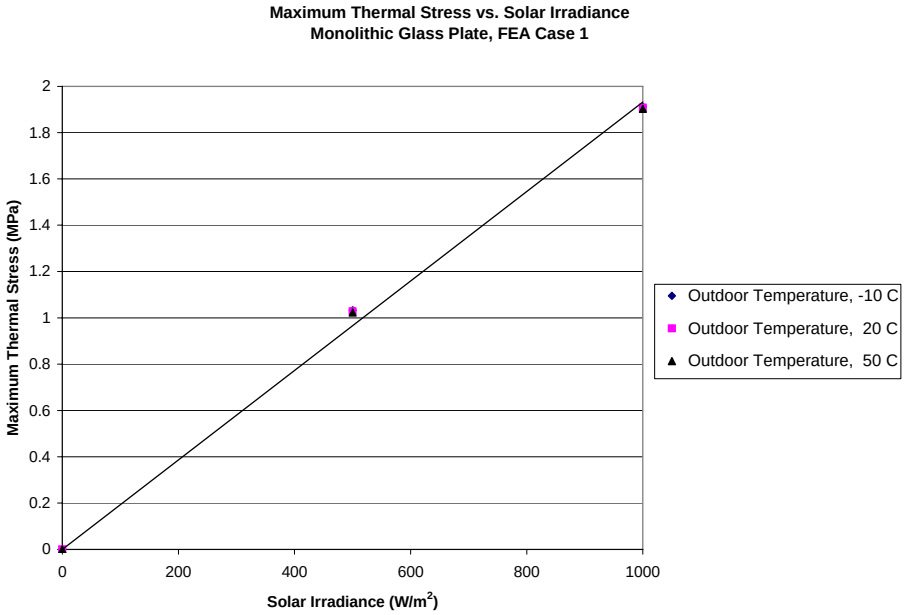

Fig. 32. Maximum thermal stress versus solar irradiance, FEA case 1, 6 mm clear monolithic glass plate

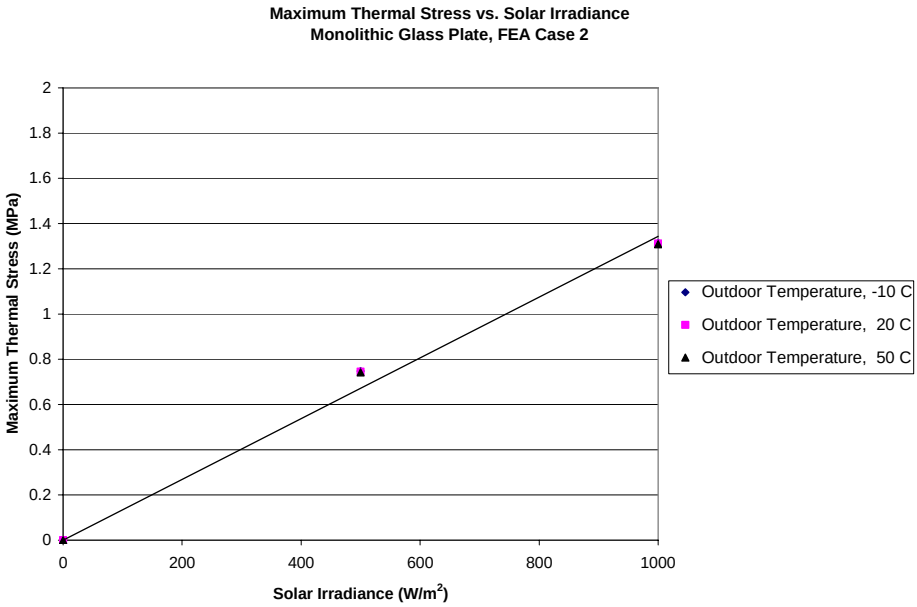

Fig. 33. Maximum thermal stress versus solar irradiance, FEA case 2, 3 mm clear monolithic glass plate

FEA case 1 (6mm) and FEA case 2 (3mm) are for clear monolithic glass plates. As shown in Figs. 32 and 33, the thermal stress is independent of outdoor temperature and increases linearly from zero with an increase in solar irradiance, which is in accordance with Beason and Lingnell (2002). Also, the initial preload thermal stress for a monolithic glass plate is found to be approximately zero.

The magnitude of the thermal stresses that can cause glass to fail depend on the glass edge condition. Thermal stresses usually do not become a consideration until the perimeter tensile stress exceeds about 7 MPa. If the perimeter tensile stress exceeds 14 MPa, serious concerns are raised about the survivability of the glass.

Results for FEA cases 1 and 2, show that the maximum thermal stress occurs when the solar irradiance is 1000 W/m^2 and results in a maximum thermal stress of 1.90 MPa and 1.33 MPa for FEA case 1 and FEA case 2, respectively. The thermal stresses for FEA

cases 1 and 2 are well below the threshold believed to be associated with thermal breakage, thus if thermal breakage were to occur in cases 1 or 2 it would more than likely be due to extremely poor edge conditions or glass impurities.

IG Unit Case Study Results

Fig. 34, illustrates the geometry of an IG unit used in the FEA analysis. The IG unit geometry consists of two single glass plates separated by a 12.93 mm air space. Each glass plate is 323.85 mm long, with a thickness t_{GL} and a 19.05 mm edge bite. The glass plates are separated by two 0.508 mm thick layers of silicone, and a 11.91 mm steel spacer. The geometry of the steel spacer is as shown in Fig. 35.

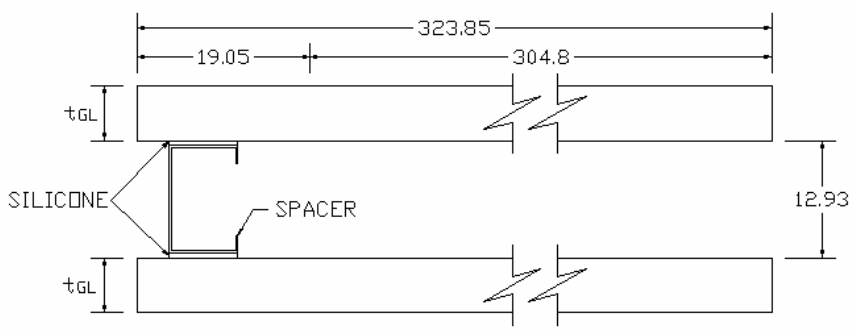

Fig. 34. IG unit geometry for FEA analysis

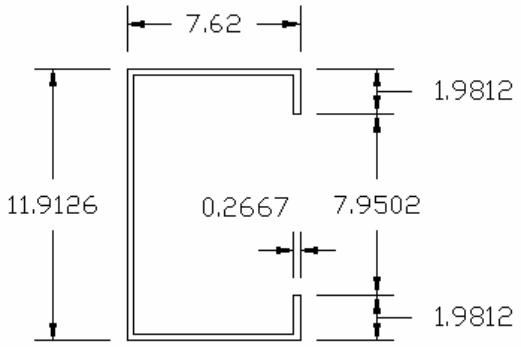

Fig. 35. Geometry of steel spacer

The IG unit mesh consists of nodes and rectangular elements as shown in Fig. 36. An illustration of the mesh used for the steel spacer is shown in Fig. 37. Once the geometry, mesh, and properties have been defined the next step is to perform the EA and TA, the results of which are presented in Figs. 38 through 43, for FEA cases 3 through 8, respectively.

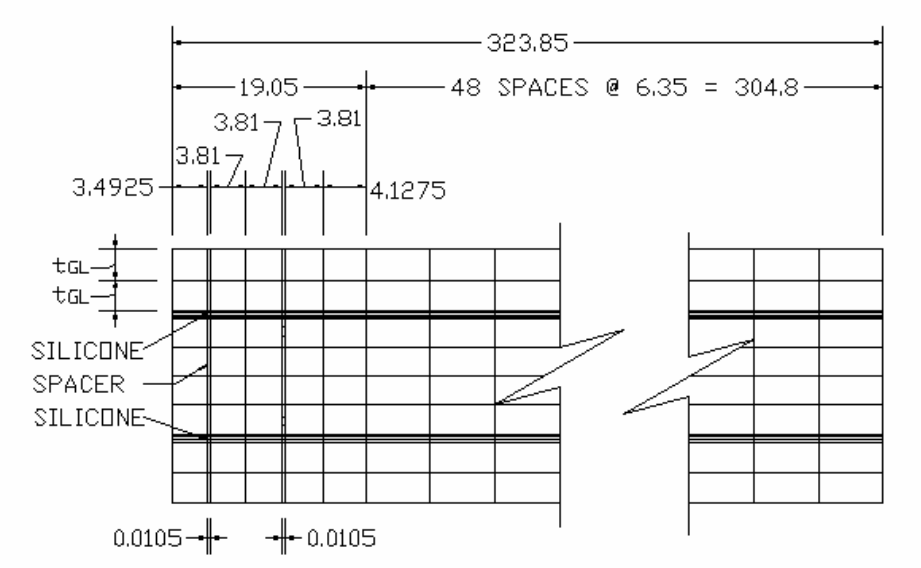

Fig. 36. Finite element mesh, IG unit

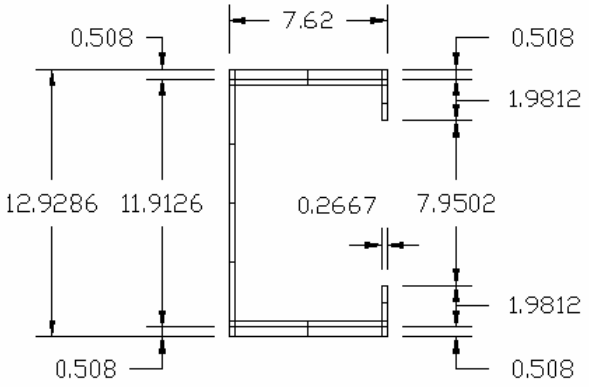

Fig. 37. Finite element mesh, steel spacer and silicone

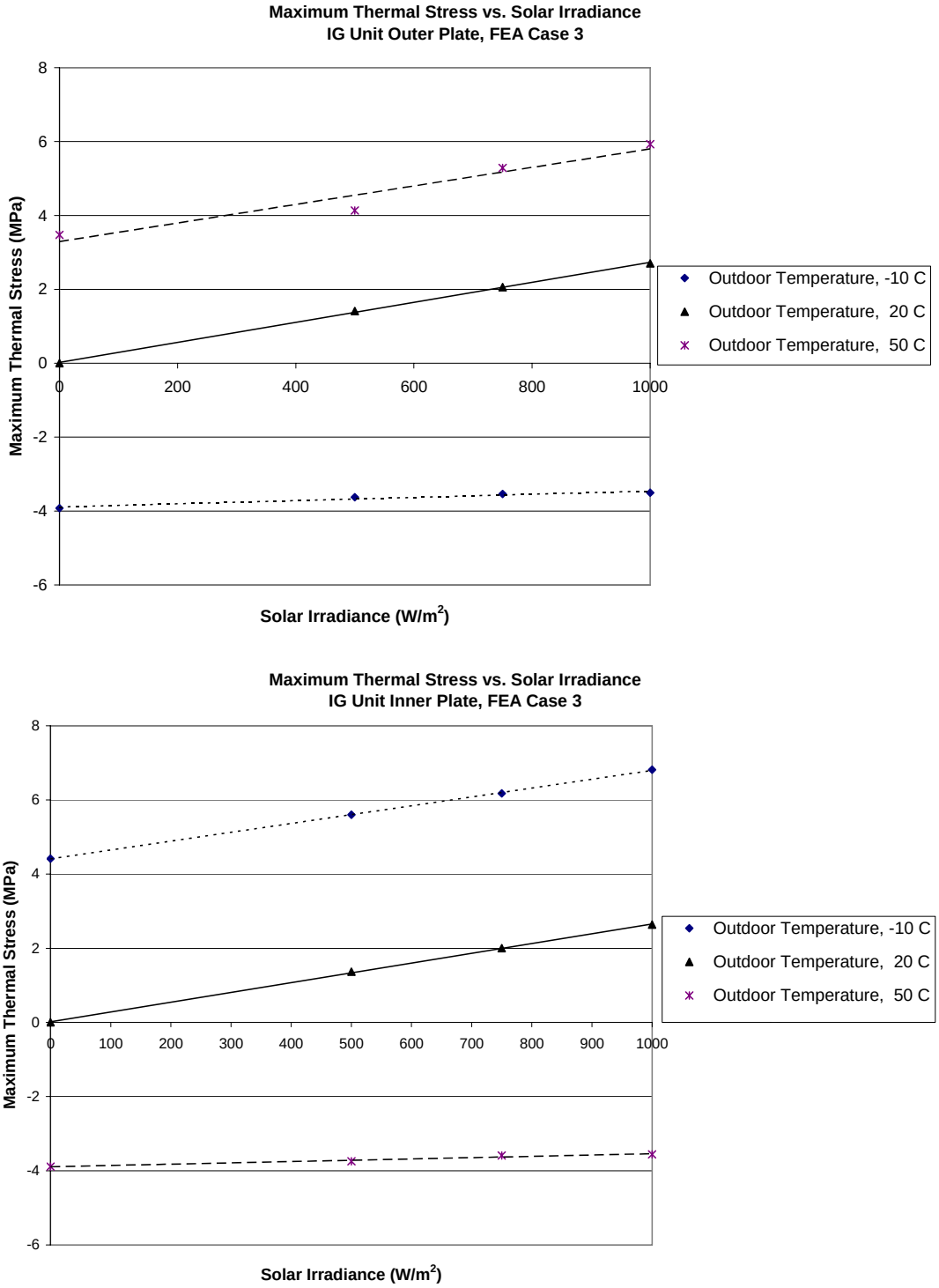

Fig. 38. Maximum thermal stress versus solar irradiance, FEA case 3 (IG unit), 6 mm clear outer plate and 6 mm clear inner plate

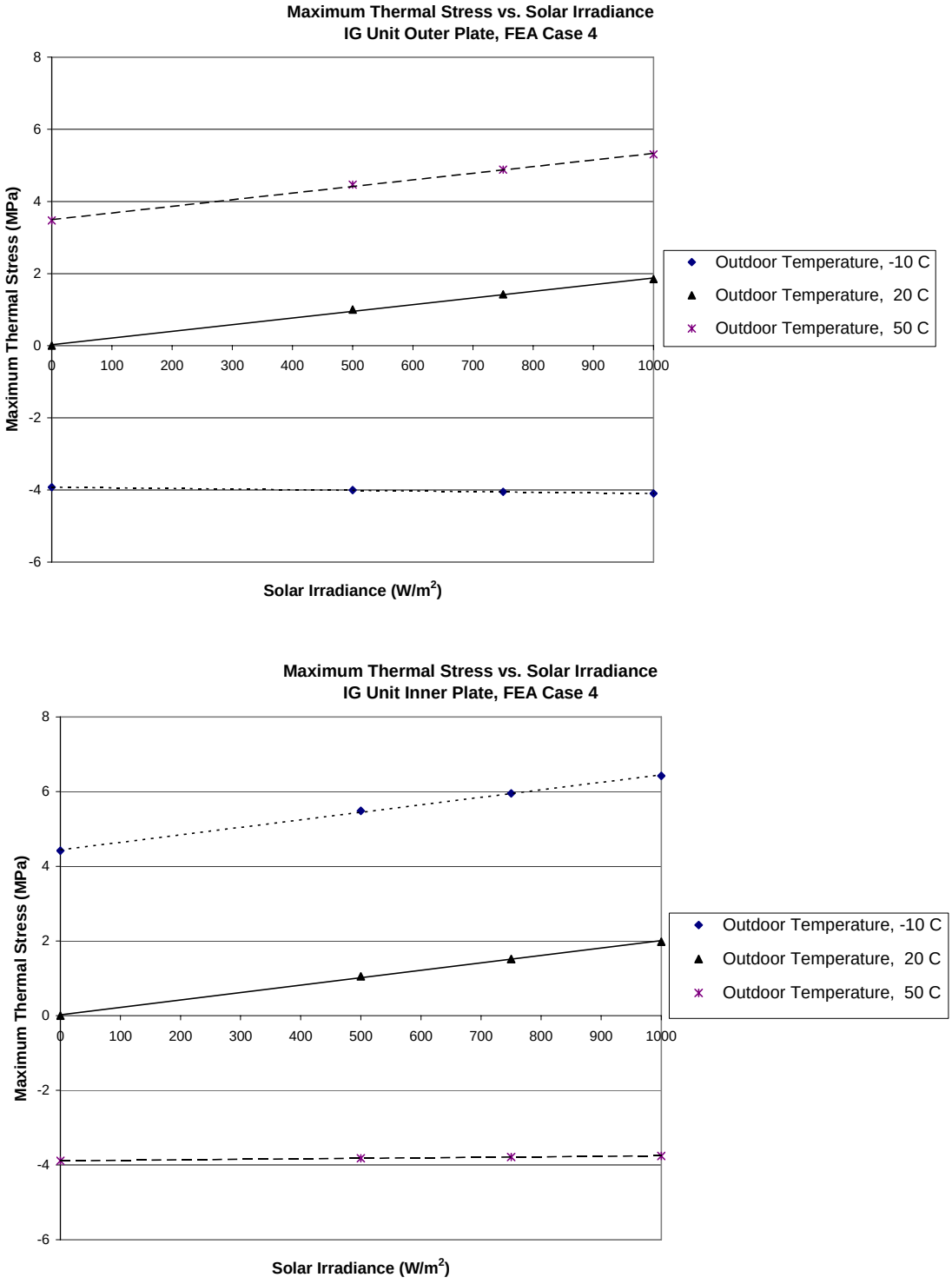

Fig. 39. Maximum thermal stress versus solar irradiance, FEA case 4 (IG unit), 3 mm clear outer plate and 3 mm clear inner plate

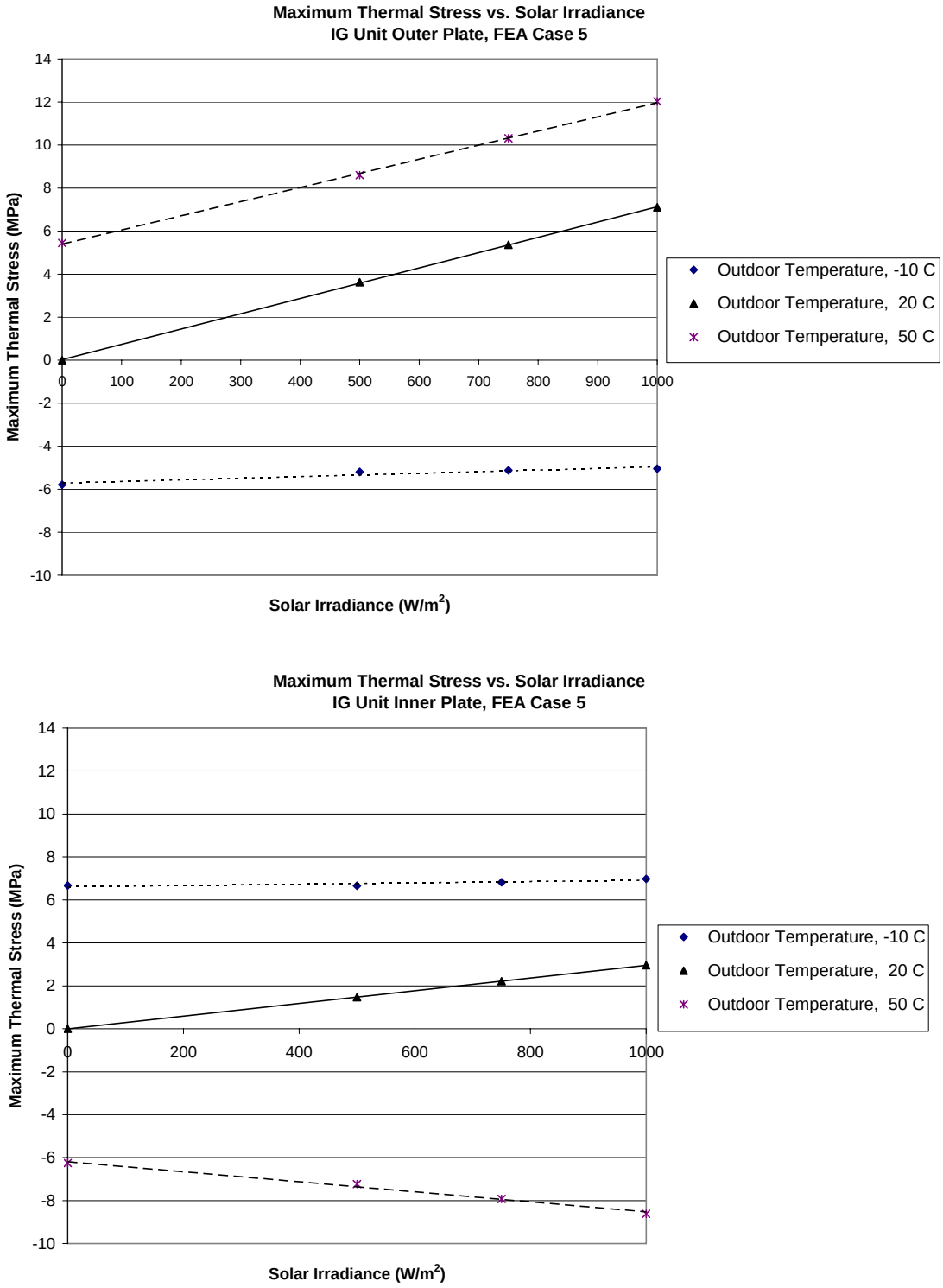

Fig. 40. Maximum thermal stress versus solar irradiance, FEA case 5 (IG unit), 6 mm clear with low-e, 2 outer plate and 6 mm clear inner plate

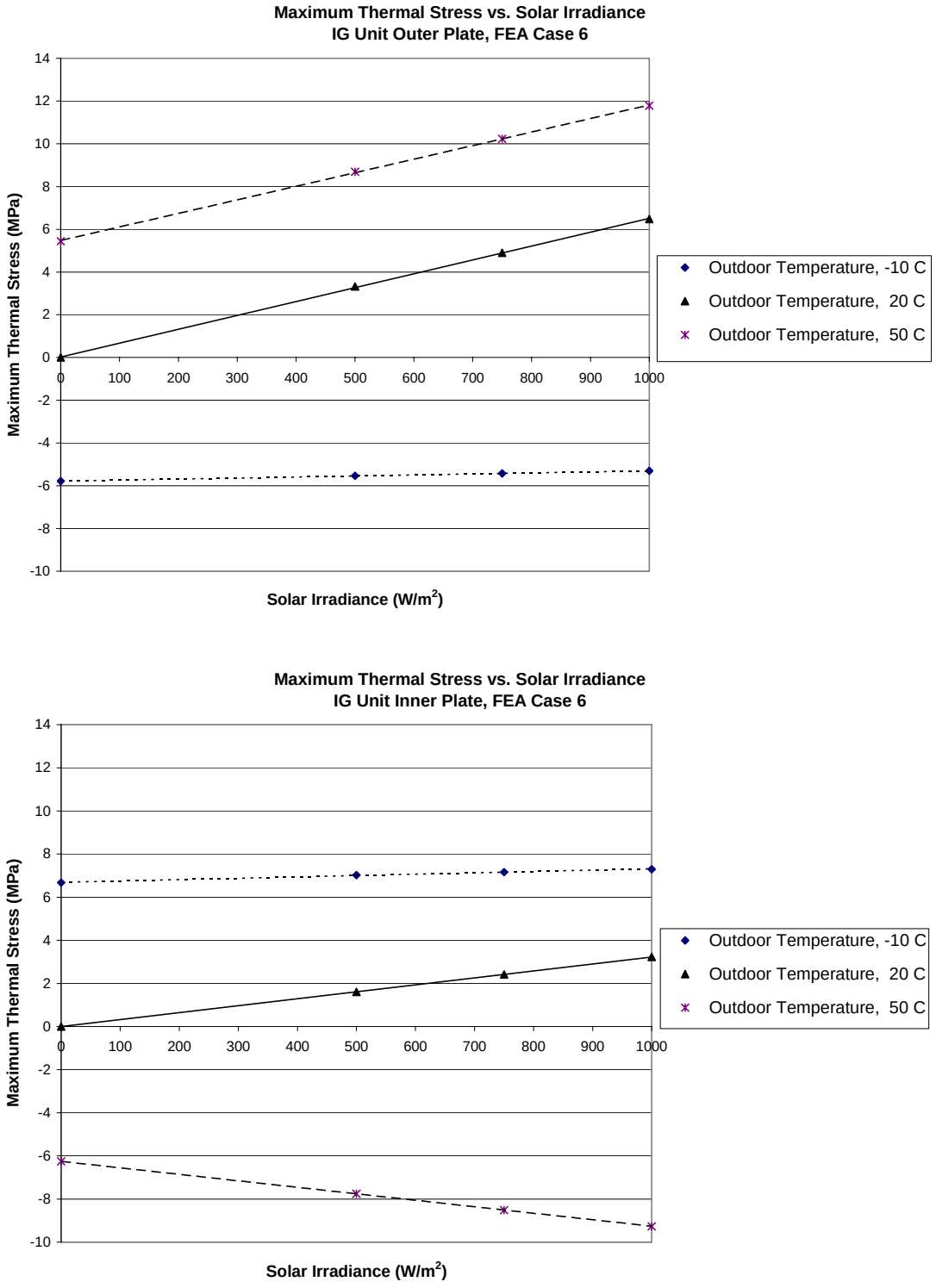

Fig. 41. Maximum thermal stress versus solar irradiance, FEA case 6 (IG unit), 3 mm clear with low-e, 2 outer plate and 3 mm clear inner plate

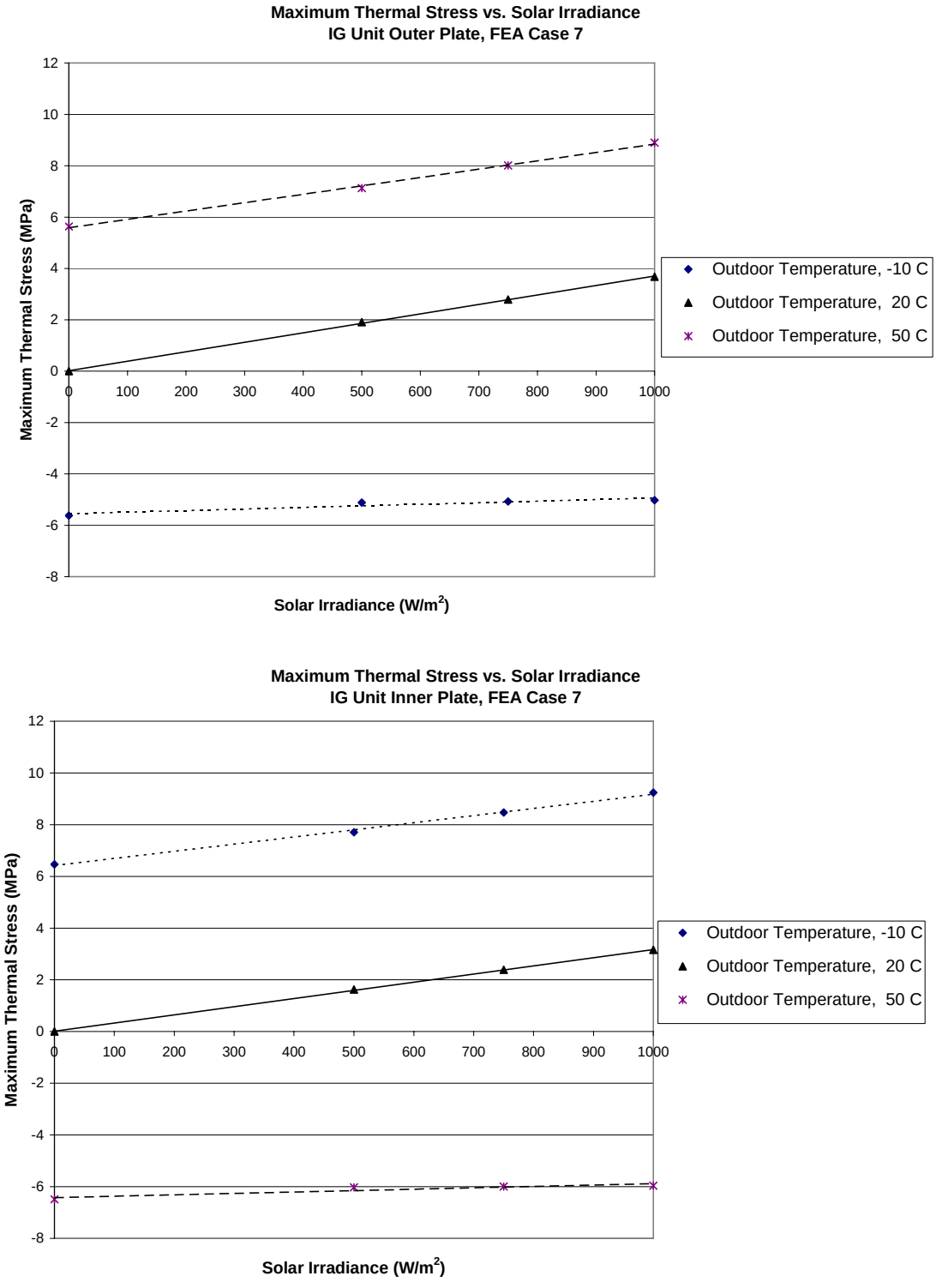

Fig. 42. Maximum thermal stress versus solar irradiance, FEA case 7 (IG unit), 6 mm clear outer plate and 6 mm clear with low-e, 2 inner plate

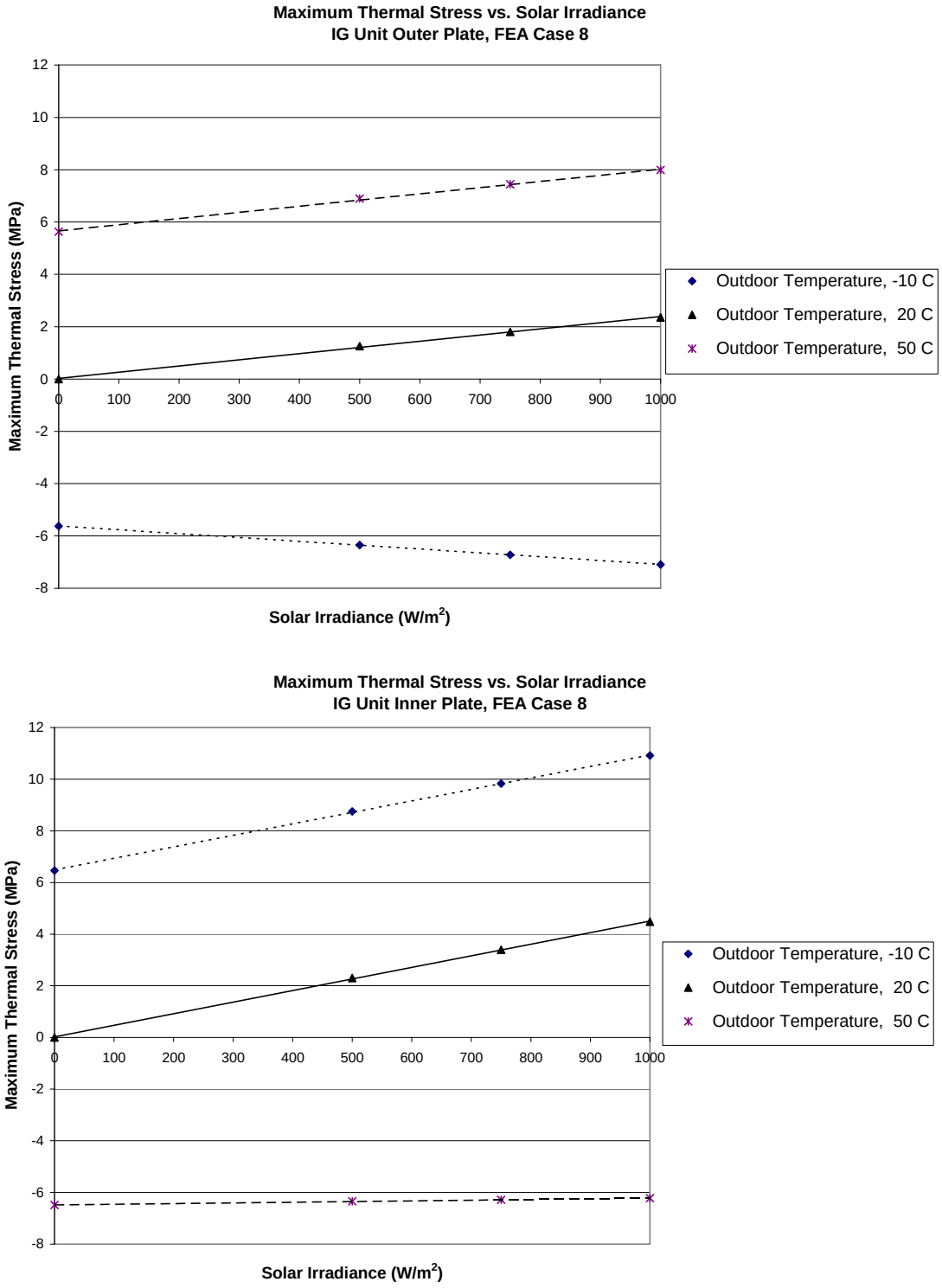

Fig. 43. Maximum thermal stress versus solar irradiance, FEA case 8 (IG unit), 3 mm clear outer plate and 3 mm clear with low-e, 2 inner plate

For FEA cases 3 through 8, the maximum thermal stress is associated with the maximum input solar irradiance (1000 W/m^2). Also for these cases, the plates have an initial pre-load thermal stress when in equilibrium with the environment, due to energy transfer through the spacer. Also, for an outdoor temperature other than 20 ^oC, if the outer plate develops tensile stresses at the perimeter of glass, the inner plate will develop compressive stresses.

FEA case 3 (6 mm) and FEA case 4 (3 mm) are for IG units with clear outer and inner glass plates. The maximum tensile stress for the inner plate occurs when the outdoor temperature is -10 ^oC and results in a maximum thermal stress of 6.81 MPa and 6.42 MPa for FEA case 3 and FEA case 4, respectively. The maximum tensile stress for the outer plate occurs when the outdoor temperature is 50 ^oC and results in a maximum thermal stress of 5.93 MPa and 5.30 MPa for FEA case 3 and FEA case 4, respectively.

FEA case 5 (6 mm) and FEA case 6 (3 mm) are for IG units with “low-e, 2” outer and clear inner glass plates. The maximum tensile stress for the inner plate occurs when the outdoor temperature is -10 ^oC and results in a maximum thermal stress of 6.98 MPa and 7.30 MPa for FEA case 5 and FEA case 6, respectively. The maximum tensile stress for the outer plate occurs when the outdoor temperature is 50 ^oC and results in a maximum thermal stress of 12.02 MPa and 11.78 MPa for FEA case 5 and FEA case 6, respectively.

FEA case 7 (6 mm) and FEA case 8 (3 mm) are for IG units with clear outer and “low-e, 2” inner glass plates. The maximum tensile stress for the inner plate occurs when the outdoor temperature is -10 ^oC and results in a maximum thermal stress of 9.24 MPa and 10.92 MPa for FEA case 7 and FEA case 8, respectively. The maximum tensile stress for the outer plate occurs when the outdoor temperature is 50 ^oC and results in a maximum thermal stress of 8.90 MPa and 7.99 MPa for FEA case 7 and FEA case 8, respectively.

As previously discussed, thermal breakage can result at stresses as low as 7 MPa. If the thermal stresses approach or exceed 14 MPa the concern for thermal breakage is significant. The maximum thermal stresses associated with FEA cases 3 and 4 that incorporate clear glass plates show that the maximum thermal stress is between 5.30 and 6.81 MPa. Based on these reported stresses it can be concluded that there is little concern for thermal breakage if the IG unit is fabricated with clear glass. The IG units in cases 5 through 8 incorporate low-e coatings, which develop the largest thermal stresses. The maximum thermal stresses in these cases are between 6.98 and 12.02 MPa; thus, thermal breakage is of great concern when low-e coatings are involved.

CHAPTER VI

CONCLUSION

Research Summary

To meet energy standards being enforced due to the concern for energy conservation, the use of high performance insulating glass (IG) units have become essential in the residential and commercial built environment. While the performance of IG units are continuously improved to reduce energy exchange with the surrounding environment, the methods used to reduce the energy flow typically increase the absorptance of the glass plate. The increased absorptance results in increased thermal stresses and can lead to thermal breakage. This has become a significant problem for window manufacturers.

The research presented herein is intended to improve understandings of how thermal stresses develop in IG units subjected to solar irradiance and to compare the thermal performance of IG units and monolithic glass plates. To accomplish this, a review of the pertinent literature was performed to establish how energy is exchanged between IG units and the surrounding environment.

Energy enters the IG unit in the form of absorbed solar irradiance. Typical energy exchange between IG units and the surrounding environment consists of conduction, forced convection, and long wave radiation on the surface facing the outdoor environment and conduction, natural convection, and long wave radiation on the surface facing the indoor environment. In addition, IG units incorporate energy exchange through the gas space cavity. The energy exchange through the gas space cavity is governed by conduction, natural convection, and long wave radiation.

The effects of conduction, convection, and long wave radiation combine mathematically in a nonlinear fashion. This complicates the numerical analysis required to predict the temperature distribution of a glass plate. ASTM 2431-06 developed for the design of monolithic glass plates linearizes the energy exchange due to conduction, convection, and long wave radiation through the use of total energy exchange coefficients. In this research it was shown that this concept could be extended to gas space cavities of IG units. This was accomplished through the development of a numerical propagation procedure.

The numerical propagation procedure results in the calculation of a single, cavity energy exchange coefficient (CEEC), which linearizes the conduction, natural convection, and long wave radiation energy exchange through IG gas spaces. It was shown that the CEEC can be used to accurately model the nonlinear energy exchange of gas space cavities. The use of the CEEC greatly simplifies the numerical analysis procedures needed to determine thermal stresses in IG glass plates.

A numerical propagation procedure to estimate the magnitude of the CEEC was implemented in a case study to determine the effect of outdoor temperature, input solar irradiance, and low-e coatings on the CEEC. Results suggest that the CEEC value increases linearly with an increase in outdoor temperature for IG units without low-e coatings and the CEEC remains relatively constant when a low-e coating is applied. The results also suggest that the CEEC value is relatively independent of the magnitude of the input solar irradiance and the location of low-e coating. The results further suggest that reducing the effective cavity emissivity, reduces the CEEC value.

A finite element parameter study that incorporated the CEEC was conducted to determine thermal stress trends in both IG units and monolithic glass plates. The parameter study was performed to determine the effect of input solar irradiance, outdoor temperature, and the type and location of the low-e coating on thermal stresses.

For the parameter study, the frame was modeled as fully insulated with an edge bite of 19.05 mm. For cases involving IG units, a steel spacer and silicone separated the outer and inner glass plates, the fill gas was air, and the low-e coating was varied between the #2 and #3 surfaces. The energy exchange through the gas space cavity was modeled using the CEEC value. The thermal stresses were assumed to be independent of aspect ratio, and the mechanical bonds between the outer and inner glass plates, the spacer, and the silicone were assumed to have minimal effect on the thermal stresses that develop in the glass plates according to Pilette and Taylor (1988).

The results suggest that IG units develop larger thermal stresses than monolithic glass plates, and low-e coatings increase the thermal stresses of IG units. This is the case because inter-reflectance takes place between the outer and inner glass plates and because low-e coatings typically increase the absorptance characteristics of IG glass plates.

The results further suggest that the maximum thermal stresses that develop in monolithic glass plates and IG units vary linearly with input solar irradiance. Thus, the maximum thermal stress for any value of input solar irradiance can be determined by performing an equilibrium analysis and a single transient analysis and connecting the two data points with a straight line. This greatly reduces the amount of calculations needed to determine the thermal stresses that develop for a given window (Wright and Sullivan 1995).

Finally, the results suggest that IG units, unlike monolithic glass plates, can develop an initial preload stress under equilibrium conditions. The preload stress occurs due to the thermal bridge effects of the spacer. In cold environmental conditions (less than 20 ^{o}C), the inner plate is warmer than the outer plate. Thus, heat from the warmer inner plate flows through the spacer to the outer plate. This increases the perimeter temperature of the outer plate and reduces the perimeter temperature of the inner plate. The net result is that the inner plate perimeter stresses are tensile while the outer plate perimeter stresses are compressive. The opposite situation occurs when an IG unit is placed in hot envi-

ronmental conditions (greater than 20 ^{o}C). In this case, the perimeter of the outside plate experiences a tensile preload, while the perimeter of the inside plate experiences a compressive preload.

Major Conclusions

The major conclusions of this research can be summarized as follows:

- The numerical propagation procedure can be used to accurately linearize the energy exchange through gas space cavities.
- Low-e coatings reduce the energy exchange through gas space cavities by reducing the flow of radiation.
- IG units are more susceptible to thermal breakage than monolithic glass plates.
- Low-e coatings increase thermal stresses in IG units.
- The maximum thermal stresses that develop in IG units and monolithic glass plates vary linearly with input solar irradiance.
- IG units develop preload stresses due to energy flow through the spacer even when no solar irradiance is involved.
- The inner plate of an IG unit is more susceptible to thermal breakage when placed in cold environmental conditions while the outer plate is more susceptible to thermal breakage when placed in hot environmental conditions.

Future Research

The gas space cavity energy exchange of IG units is governed by conduction, natural convection, and long wave radiation. A low-e coating is used to reduce the effective emissivity of the cavity which ultimately reduces the radiation flow between the outer and inner plates of an IG unit. Similarly, various gases can be implemented in IG units to reduce the energy flow due to conduction and natural convection. In addition, IG unit

glass plates can incorporate tints that are used to block or transmit parts of the solar spectrum. Therefore, future research is needed to determine the effect of various cavity emissivities, fill gases, and tints on IG thermal stresses.

The parameter study was conducted with a fully insulated frame in accordance with ASTM 2431-06. In this case, it is assumed that energy is not transferred between the frame and the glass. Also, for cases involving IG units, the parameter study modeled a steel spacer. There are many different frame and spacers types in common use. Therefore, future research should evaluate the effects of different frame types and spacers on the development of IG thermal stresses.

The parameter study focused only on solar irradiance as a heat input mechanism. However, experience suggests that heat can be input into a glass plate from other sources such as heating registers, intense indoor lighting, etc. Further there are other factors that influence the development of thermal stress in glass plates such as shadows, indoor energy traps such as Venetian blinds and curtains, etc. Further research is needed to evaluate the other mechanisms that effect the development of thermal stresses.

REFERENCES

ALGOR Finite Element Analysis Software (ALGOR). (2003). Version 13.30, Pittsburgh, PA.

American Society of Heating, Refrigerating and Air-Conditioning Engineers (ASHRAE). (2005). *ASHRAE handbook, fundamentals*, Atlanta, GA.

American Society for Testing and Materials (ASTM). (2006). "Standard practice for determining the resistance of single glazed annealed architectural flat glass to thermal loadings." *ASTM Standard, Designation: E 2431-06*, Philadelphia.

Beason W. L. and Lingnell A. W. (2002). "A thermal stress evaluation procedure for monolithic glass." *ASTM special technical publication*, 1434, 105-118.

Datta, A. K. (2002). *Biological and bioenvironmental heat and mass transfer*, Marcel Dekker, New York, NY.

Duffie, J. A. and Beckman, W. A. (1974). *Solar energy thermal processes*, John Wiley & Sons, New York, NY.

Elder, J. W. (1965). "Turbulent free convection in a vertical slot." *Journal of Fluid Mechanics*, 23, 99-111.

El Sherbiny, S. M., Hollands, K. T., and Raithby, G. D. (1982). "Effect of thermal boundary conditions on natural convection in vertical and inclined air layers." *Journal of Heat Transfer*, 104, 515-520.

Finlayson, E., Arasteh, D., Huizenga, C., and Rubin, M. (1993). "WINDOW 4.0: documentation of calculation procedures." <http://www.otsi.gov/bridge/product.biblio.jsp?osti_id=10112503> (Retrieved on May 17, 2007).

Gordon, J. (2001). *Solar energy, the state of the art*, James & James, London, UK.

Gustavsen, A., Arasteh, D., Kohler, C. and Curcija, D. (2005). "Two-dimensional conduction and CFD simulations of heat transfer in horizontal window frame cavities." *ASHRAE Transactions*, 111, 587-598.

Han, B. and Muneer, T. (1996). "Multiple glazed windows: design charts." *Building Services Engineering Research and Technology*, 17, 223-229.

Ismail, K. R. and Henriquez, J. R. (2005). "Two-dimensional model for the double glass naturally ventilated window." *International Journal of Heat and Mass Transfer*, 48, 461-475.

Kennedy, J. B. (1976). *Basic statistical methods for engineers and scientists, second edition*, Thomas Y. Crowell Company, New York, NY.

Manz, H. (2003). "Numerical simulation of heat transfer by natural convection in cavities of facade elements." *Energy and Buildings*, 35, 305-311.

Muneer, T. Abodahab, N., and Han, B. (1996). "Gas flow in window enclosures and its effect on temperature distribution." *Advances in Fluid Mechanics*, 9, 233-242.

Muneer, T., Abodahab, N., and Gilchrist A. (1997). "Combined conduction, convection, and radiation heat transfer model for double-glazed windows." *Building Services Engineering Research and Technology*, 18, 183-191.

Muneer, T., Abodahab, N., Weir, G., and Kubie, J. (2000). *Windows in buildings*, Architectural Press, Woburn, MA.

Pilkington (2005). ATS-123, "Thermal stress." <http://www.pilkington.com/the+americas/usa/english/building+products/ats+bulletins/ default.htm > (Retrieved on April 25, 2007).

Pilette, C. F. and Taylor D. A. (1988). "Thermal stresses in double-glazed windows." *Canadian Journal of Civil Engineering*, 15, 807-814.

Powles, R., Curcija, D., and Kohler, C. (2002). "Solar Absorption in thick and multilayered glazings." <http://www.osti.gov/bridge/purl.cover.jsp?purl=/806104-MD0-cbS/native/> (Retrieved on May 17, 2007).

Raithby, G. D., El Shrebiny, S. M., and Hollands, K. T. (1982). "Heat transfer by natural convection across vertical and inclined air layers." *Journal of Heat Transfer*, 104, 96-102.

Rubin, M. (1982). "Calculating heat transfer through windows." *Energy Research*, 6, 341-349.

Thomas, L. C. (1992). *Heat transfer*, Prentice-Hall, Edgewood Cliffs, NJ.

Turner, D. P. (1977). *Window glass design guide*, Nichols, New York, NY.

Wijeysundera, N. E. (1975). "A net radiation method for the transmittance and absorptivity of a series of parallel regions." *Solar Energy*, 17, 75-77.

Wright, J. L. and Sullivan, H. F. (1995). "A two-dimensional numerical model for glazing system thermal analysis." *ASHRAE Transactions*, 101, 819-831.

Wright, J. L. (1996). "A correlation to quantify convective heat transfer between vertical window glazings." *ASHRAE Transactions*, 102, 940-946.

Wright, J. L. (1998). Calculating center-glass performance indices of windows." *ASHRAE Transactions*, 104, 1230-1241.

Wright, J. L. and Barry, C. B. (1999). "A new approach to perimeter of glass temperature prediction and its application to predicting thermal breakage in insulated glazing units." *ASHRAE Transactions*, 105, 909-917.

Zhong-wei, L., Jia-lin, S., and Yan-ruo, H. (1999). "Thermal stress and fracture of building glass." *Glass Technology*, 40, 191-194.

VITA

Jeremy Wayne Klam
Texas A&M University
Zachry Department of Civil Engineering
3136 TAMU
College Station, TX 77843-3136
jklam@neo.tamu.edu

Jeremy Wayne Klam received his B.S. degree in civil engineering from Texas A&M University in August 2005. After graduating, he began work at Texas A&M University towards a M.S. degree in civil engineering. He worked for the Texas Transportation Institute (TTI) through the duration of his undergraduate and graduate education. While employed with TTI, the majority of his time was spent as a draftsman; he also participated in the design and analysis of new roadway safety devices. Mr. Klam received his M.S. degree in August 2007. He is currently employed with Mustang Engineering in Houston, Texas, where he does steel and concrete design for the oil refinery industry.